COMPILATION OF ROCK PROPERTIES FROM FORGE WELL 58-32, MILFORD, UTAH

by Mark Gwynn[1], Rick Allis[1], Christian Hardwick[1], Clay Jones[2], Peter Nielsen[1], and Will Hurlbut[1]

[1]Utah Geological Survey, Salt Lake City, Utah
[2]Energy & Geoscience Institute, University of Utah, Salt Lake City, Utah

Miscellaneous Publication 169-L
Utah Geological Survey
a division of
UTAH DEPARTMENT OF NATURAL RESOURCES

This paper is part of *Geothermal Characteristics of the Roosevelt Hot Springs System and Adjacent FORGE EGS Site, Milford, Utah*. https://doi.org/10.34191/MP-169

Bibliographic citation:

Gwynn, M., Allis, R., Hardwick, C., Jones, C., Nielsen, P., and Hurlbut, W., 2019, Compilation of rock properties from FORGE well 58-32, Milford, Utah, *in* Allis, R., and Moore, J.N., editors, Geothermal characteristics of the Roosevelt Hot Springs system and adjacent FORGE EGS site, Milford, Utah: Utah Geological Survey Miscellaneous Publication 169-L, 36 p., https://doi.org/10.34191/MP-169-L.

COMPILATION OF ROCK PROPERTIES FROM FORGE WELL 58-32, MILFORD, UTAH

by Mark Gwynn, Rick Allis, Christian Hardwick, Clay Jones, Peter Nielsen, and Will Hurlbut

ABSTRACT

Well 58-32 was drilled to a depth of 7536 feet in the Milford FORGE area during the summer of 2017 to confirm the reservoir characteristics inferred from over 100 existing wells and a wide variety of both new and legacy geologic and geophysical data. Drill cuttings were collected and described at 10-foot intervals and a robust suite of geophysical and image logs were run. Thermal conductivity, density, x-ray diffraction, magnetic susceptibility, and spectral gamma ray measurements were performed on the cuttings at least every 100 feet, and these analyses show that the basement rock within the FORGE area consists of a suite of intrusive rock types that are primarily granitic. Other mafic rock types were also encountered (mainly monzodiorite and a lesser volume of diorite), as was a significant volume of rock with a more intermediate composition. The laboratory analyses were used to calibrate gamma ray and density log responses, allowing foot-scale variations in rock type to be more accurately identified and interpreted throughout the well bore. Similar small-scale compositional changes can be seen in outcrop at many locations in the adjacent Mineral Mountains. The density of the granite and intermediate rock types typically ranges from 2.54 to 2.65 g/cm^3, but the higher gamma response of the granitic rock (140–290 gAPI) can often differentiate granitic compositions from intermediate compositions (70–210 gAPI). The higher density (2.65–2.90 g/cm^3) and lower gamma values (50–80 gAPI) of the dioritic compositions is more distinctive and greatly simplifies identification. The laboratory analyses and geophysical logs of the 58-32 well prove it was drilled into low porosity/low permeability intrusive rock with temperatures well within the U.S. Department of Energy-specified window of 175°–225°C. Despite small-scale compositional changes, the geomechanical characteristics throughout the reservoir zone are reasonably consistent and are suitable for testing the techniques and technologies required to develop enhanced geothermal reservoirs.

INTRODUCTION

Well 58-32 is the resource-proving well for the Milford Frontier Observatory for Research in Geothermal Energy (FORGE) project. The well was drilled in Section 32, Township 26 South, Range 9 West, Salt Lake Base Line and Meridian (SLB&M), in Milford Valley about 2 miles west of the Mineral Mountains (Figure 1). The 58-32 well was sometimes referred to as MU-ESW1 in earlier literature (Balamir and others, 2018). This report examines the physical properties of the rock in well 58-32 and several nearby wells to characterize the reservoir and to provide the criteria for recognizing intrusive rock-type variations using wireline logs in future FORGE wells. Many of the physical properties established in this report will provide a basis for the rock property assumptions required in future models and simulations of thermal, fluid flow, and geomechanical behavior.

The 58-32 well is located above the planned "toe" of the deviated wells that will be drilled in the final phase of the FORGE project. The Kenai Drilling crew, under the direction of Geothermal Resources Group, began assembling Rig 10 in late July and spudded the well at 23:30 on July 31, 2017 (Figure 2). A 17.5-inch bit was used to a depth of 342 feet, where 13-3/8-inch casing was set. A 12.25-inch bit was then used until 2180 feet was reached and 9-5/8-inch casing was set. Twelve 8.75-inch bits were then used to reach the final total depth (TD) of 7536 feet. Four temperature logs, run approximately 6 hours apart, were obtained at an intermediate depth of 6800 feet to ensure that the U.S. Department of Energy (DOE)-specified minimum temperature of 175°C would be met. A robust set of wireline logs and a Formation Micro-Imager (FMI) log were run from the shoe of the surface casing at 2173 feet to TD. The bottom of the hole was then filled with mud and gravel to protect the formation while 7-inch casing was run to 7378 feet and cemented. The shoe was subsequently drilled, and the hole was cleaned out, creating a 158 foot open-hole completion to facilitate a formation evaluation test. A second image log was then run to assess the results in the open-hole section after the formation evaluation test. Another temperature log was run 37 days after well completion to assess the near-equilibrium thermal regime prior to the end of the project phase in early 2018. A final temperature log was run slightly over one year later, during the next phase of the project, to assess the fully re-equilibrated formation temperature. Nadimi and others (2018) and Jones and others (2018, 2019) detail the formation evaluation testing, FMI logs, and the petrographic analyses of cuttings and core samples. Allis and others (2018a, 2018b) discuss the temperature logs and the FORGE thermal regime in detail.

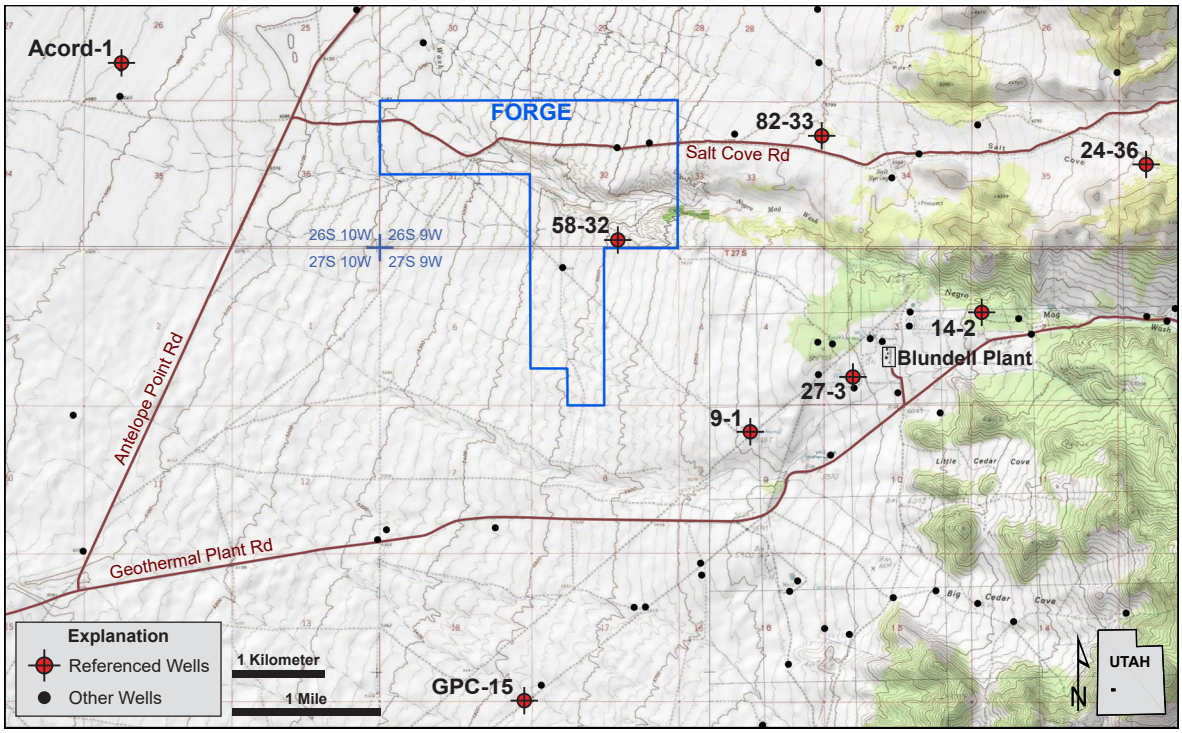

Figure 1. *Topographic base map showing the FORGE area and location of nearby wells. Well 58-32 was drilled as part of the FORGE program in the late summer of 2017. Other labeled wells are discussed in the text.*

Figure 2. *Kenai Rig 10 on the 58-32 well pad. Photograph taken on September 3, 2017, during the running of temperature logs at an intermediate depth of 6800 feet.*

FORGE WELL 58-32 DRILLING DATA

Drill Rate

The drilling rate greatly fluctuated in the near surface of the basin-fill section, sometimes approaching 1000 feet/hour for short durations, before decreasing through the rest of the section. The average drilling rate in the basin fill was 82 feet/hour. In the basement rock, below about 3176 feet, the drilling rate was less variable, and the average was around 14 feet/hour. In general, there was a steady decrease in drilling rate with increasing depth (Figure 3). However, some rate fluctuations were observed at many depths and the overall rate from about 4500 feet to TD slightly increased. Localized and sudden increases in drilling rate occurred at the transitions to smaller hole diameters (17.5-inch to 12.25-inch at 342 feet and 12.25-inch to 8.75-inch at 2180 feet). Some other increases can be correlated to changing out worn bits, as the worn bits often contributed to a decreasing trend in the drilling rate (all bit changes within a given size were in the lower part of the well where only 8.75-inch bits were used). Many other fluctuations, particularly those "spikes" of very short period (on the order of less than 10 feet of depth), may indicate small fracture zones, rock type variability, or other factors of diminishing effects. Other data show thin zones of differing rock types. Such zones may have had the greatest effect on localized drilling rates.

Weight on Bit

The trends shown for weight on bit (WOB) generally correlate to those of the drilling rate (Figure 3). The WOB occasionally exceeded 30,000 pounds in the basin-fill section, with an average of about 16,000 pounds. Weight on bit was much higher in the granitic basement section, sometimes exceeding 40,000 pounds, with an average of 28,000 pounds. The bottom part of the well, below about 4600 feet, required a much higher WOB to maintain optimal drilling rates. Weight on

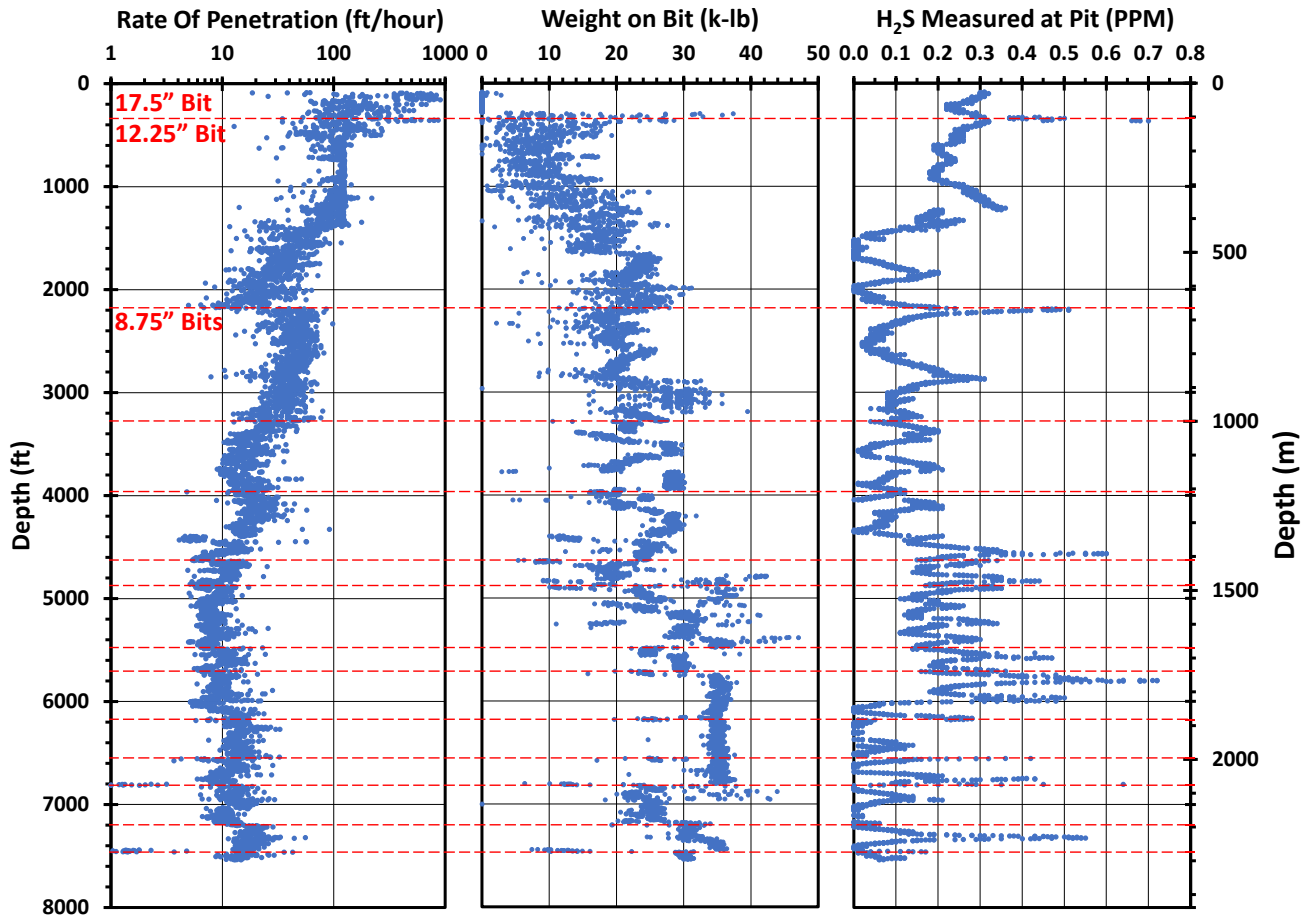

Figure 3. *Drilling data consisting of the rate of penetration and the corresponding weight on the drill bit are shown in the two graphs to the left. Drilling rate was affected primarily by changes in bit size, bit condition, and rock type. The graph on the right shows the concentration of hydrogen sulfide (H_2S) gas detected in the pit. The concentration was well below safe limits and the spikes are typically related to periods of extended circulation without drilling, prior to deviation surveys or bit changes. Red dashed lines indicate bit changes except for short core intervals at 6800 feet and 7440 feet.*

bit and rotational rate are major parameters that control the optimal drilling rate, although the use of a mud motor for much of the deeper drilling as well as the need to slide/rotate for directional control (keeping the wellbore relatively straight and vertical) are additional factors.

Hydrogen Sulfide

A low concentration of hydrogen sulfide (H_2S) gas was regularly detected in the cuttings pit, but the concentration was generally well below 0.5 parts per million (ppm) and never exceeded 0.73 ppm (the acceptable ceiling concentration for employee exposure is 20 ppm; OSHA, 2018). Hydrogen sulfide gas is a naturally occurring and colorless gas that can be trapped in sediments or dissolved in subsurface fluids, so it is commonly encountered during deep drilling operations (Cenovus Energy, 2014). Although drilling through fracture zones that contain H_2S can produce spikes, it appears that most of the spikes in Figure 3, particularly those with the greatest amplitudes, coincide with bit changes or periods of extended mud circulation (not active drilling) that allowed the H_2S concentration to build up. Additionally, fracture zones that could infuse the wellbore with H_2S might contribute to losses of drilling fluid, but no losses were recorded at any time during the drilling. Therefore, any fracture zones infusing H_2S gas into the wellbore are likely to have small apertures and poor connectivity. While localized increases in drilling rate may indicate fracture zones, they do not typically correlate with the H_2S spikes. A notable exception is the H_2S spike from about 7290 to 7360 feet. This interval was penetrated during a 12-hour period of continuous drilling and correlates with an increase in drilling rate. The FMI logs confirm that many moderately to steeply dipping fractures are present in this depth range, so it is possible that fractures in this zone were contributing H_2S. Because small quantities of H_2S are vented at the nearby Blundell geothermal plant (Figure 1), it is possible, though unlikely, that favorable wind conditions could artificially increase the detected concentration at the 58-32 well pad.

WIRELINE LOGGING DATA AND INTERPRETATIONS FROM EXISTING WELLS

Wireline logs from several existing wells were digitized and analyzed to help characterize the subsurface lithology in the FORGE area and provide insight to the lateral variability in rock properties. Examples for the Acord-1, 9-1, 14-2, and 82-33 well logs are shown in Figures 4 through 7 and well locations are shown in Figure 1.

Smoothed logs from the 82-33 and 9-1 wells (about 1.6 miles northeast and southeast of 58-32, respectively) reveal that several general rock types can be identified largely by characteristic responses of density and gamma log tools (Figures 8 through 10). In these cases, the gross lithology has been interpreted as granite, granodiorite, and diorite (or possibly monzodiorite), here called granitic, granodioritic, or dioritic. Granite will typically exhibit a high gamma response of around 150 gAPI or more and a density of about 2.67 g/cm^3. Granodiorite will have a density very similar to granite, but will show an intermediate gamma response of about 75–150 gAPI. In contrast, diorite will typically show low gamma responses of less than 75 gAPI and higher densities of around 2.8 to 3.0 g/cm^3. Sonic velocity also tends to be higher in diorite compared to the more granitic rock types, but also tends to increase with depth. Resistivity logs are less useful for identifying these intrusive rock types, but can reveal weathering and alteration zones.

The gross lithology identified at log-scale often fails to highlight small-scale, but significant, variations in rock type. For example, carefully examining the interval between 2300 and 2900 feet in the 9-1 well, which is well within the high density/low gamma "dioritic" zone, shows a large interval where the predominant diorite is interspersed with low density/high gamma granitic veins having thicknesses of less than about 30 feet, a uniform granite section of about 80 feet, and an interval that appears to be predominantly granodiorite that is about 40 feet thick (Figures 9 and 10). These small-scale variations can be seen in logs from many other wells and numerous outcrops where small intrusions of one or more rock types are present (Figure 11).

FORGE WELL 58-32 WIRELINE LOGGING DATA

Temperature Logs

Four temperature logs were run over a period of about 24 hours at an intermediate depth of 6800 feet prior to the first coring run. These logs were completed on September 3–4, 2017. A fifth logging run was made to the final TD of 7536 feet on November 2, 2017. A final logging run to TD was made on November 8, 2018. All temperature logging was accomplished by Di Drill Survey Services.

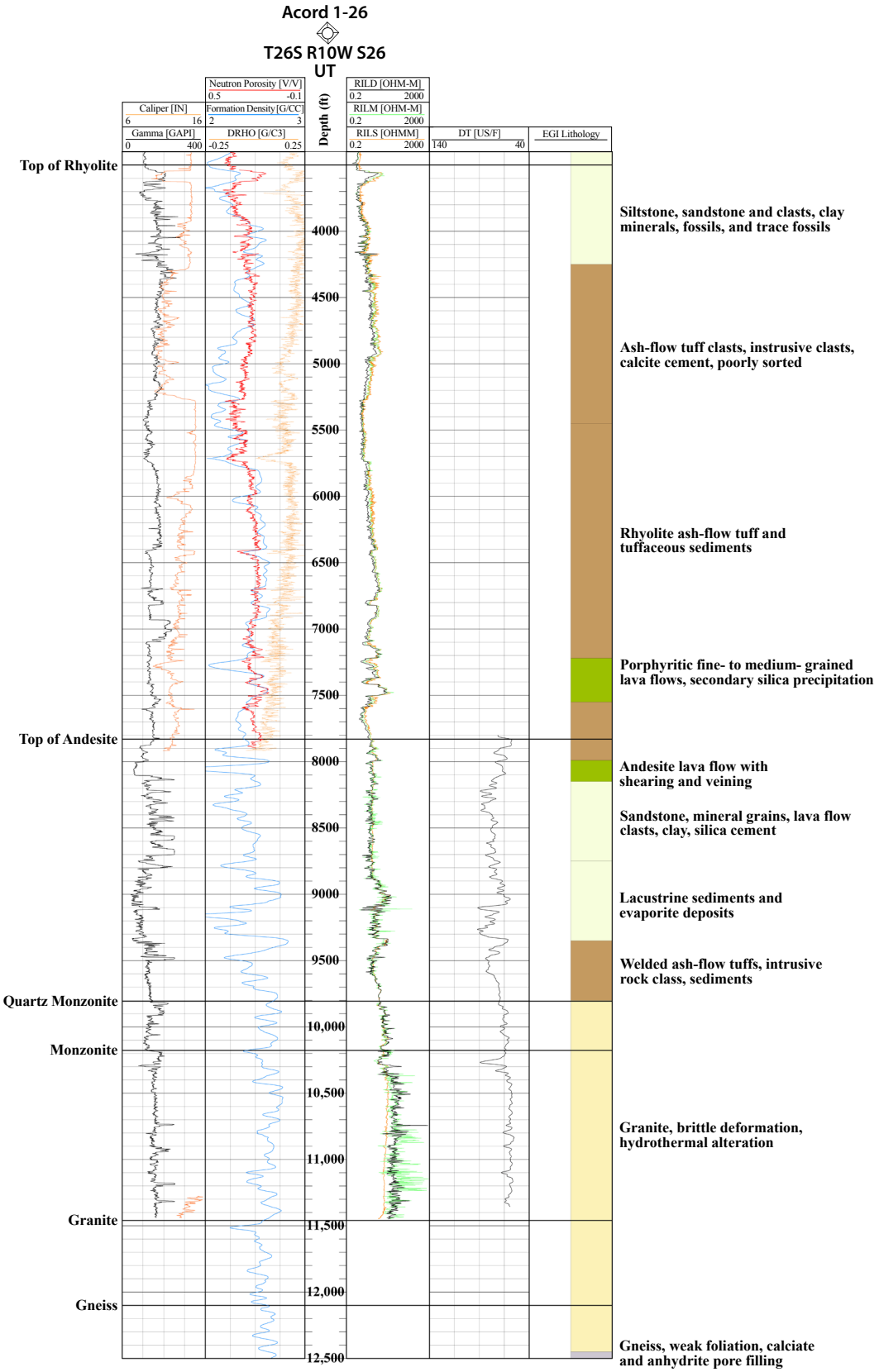

Figure 4. *Selection of wireline log responses for the Acord-1 well. "Caliper" indicates hole diameter, "Gamma" indicates natural gamma radiation, "Neutron Porosity" indicates rock porosity, "Formation Density" indicates rock density, "DRHO" indicates the quality of the density data, "RIL_" indicates rock resistivity, and "DT" indicates sonic properties of the formation. Interpreted lithology from x-ray diffraction and petrographic analyses (Jones and Moore, 2016) are shown on the right. Unlike other deep wells detailed in this report, Acord-1 has a thick sedimentary and volcanic sequence above the granitic basement.*

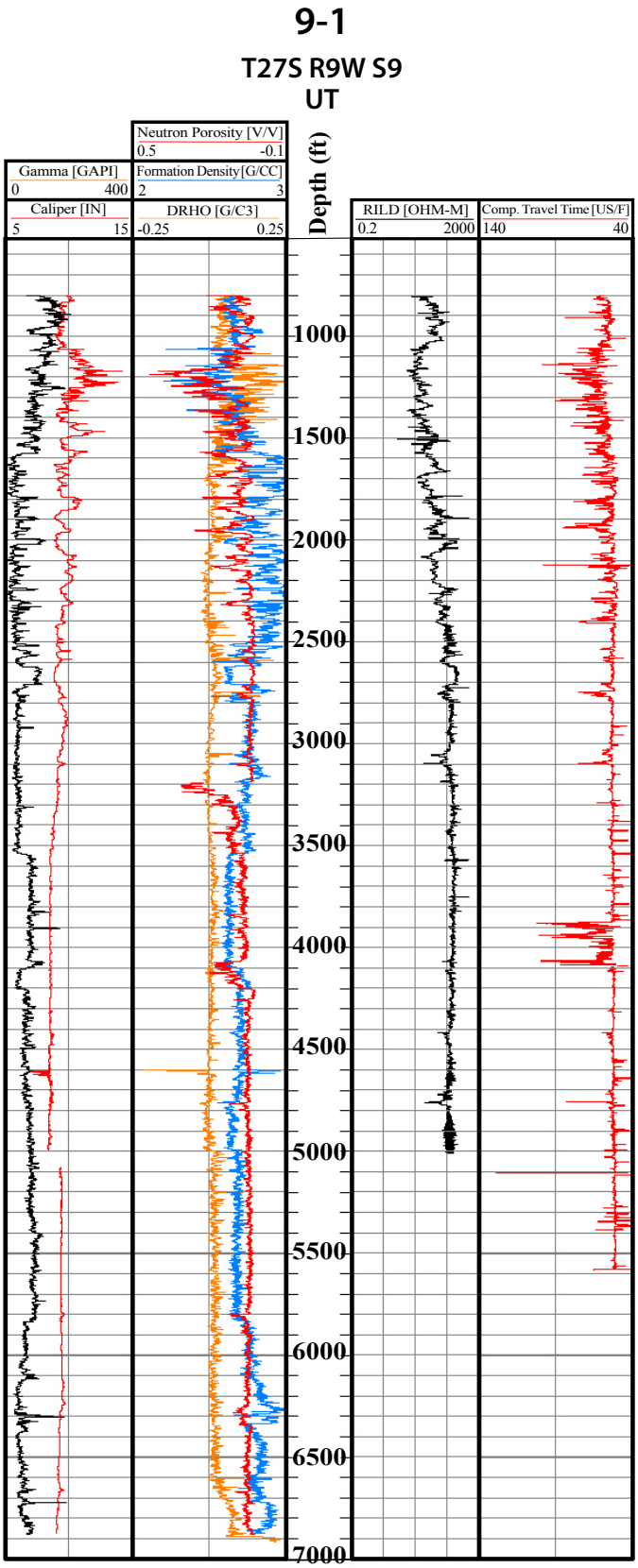

Figure 5. *Selection of wireline log responses for well 9-1. "Caliper" indicates hole diameter, "Gamma" indicates natural gamma radiation, "Neutron Porosity" indicates rock porosity, "Formation Density" indicates rock density, "DRHO" indicates the quality of the density data, "RILD" indicates rock resistivity, and "Comp Travel Time" indicates sonic properties of the formation. The gamma and formation density curves are the most useful for identifying intrusive rock types in the well. High gamma/low density responses are characteristic of granitic rocks while low gamma/high density responses are characteristic of dioritic rocks.*

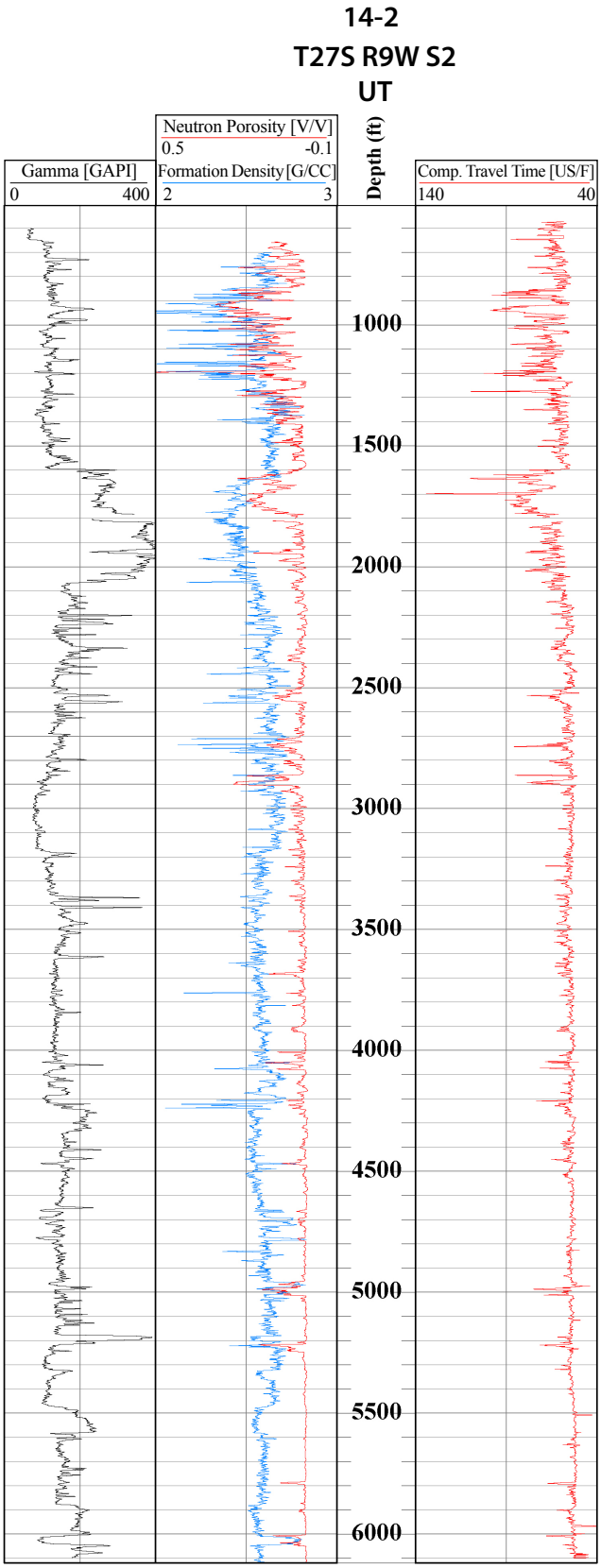

Figure 6. *Selection of wireline log responses for well 14-2. "Gamma" indicates natural gamma radiation, "Neutron Porosity" indicates rock porosity, "Formation Density" indicates rock density, and "Comp Travel Time" indicates sonic properties of the formation. The gamma and formation density curves are the most useful for identifying intrusive rock types in the well. High gamma/low density responses are characteristic of granitic rocks while low gamma/high density responses are characteristic of dioritic rocks.*

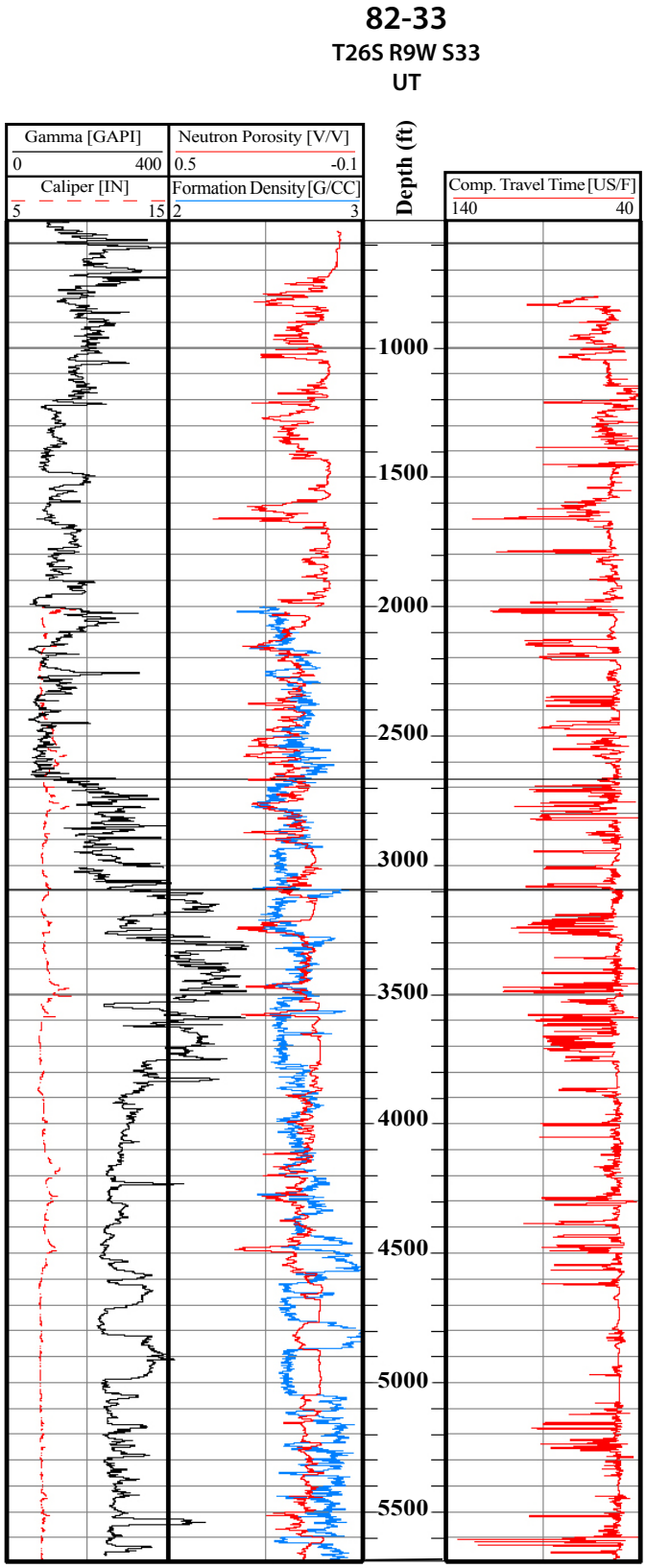

Figure 7. *Selection of wireline log responses for well 82-33. "Caliper" indicates hole diameter, "Gamma" indicates natural gamma radiation, "Neutron Porosity" indicates rock porosity, "Formation Density" indicates rock density, and "Comp Travel Time" indicates sonic properties of the formation. The gamma and formation density curves are the most useful for identifying intrusive rock types in the well. High gamma/low density responses are characteristic of granitic rocks while low gamma/high density responses are characteristic of dioritic rocks. Velocity logs are sensitive to borehole conditions, which is the cause of most of the "spikes" in the "Comp Travel Time" log.*

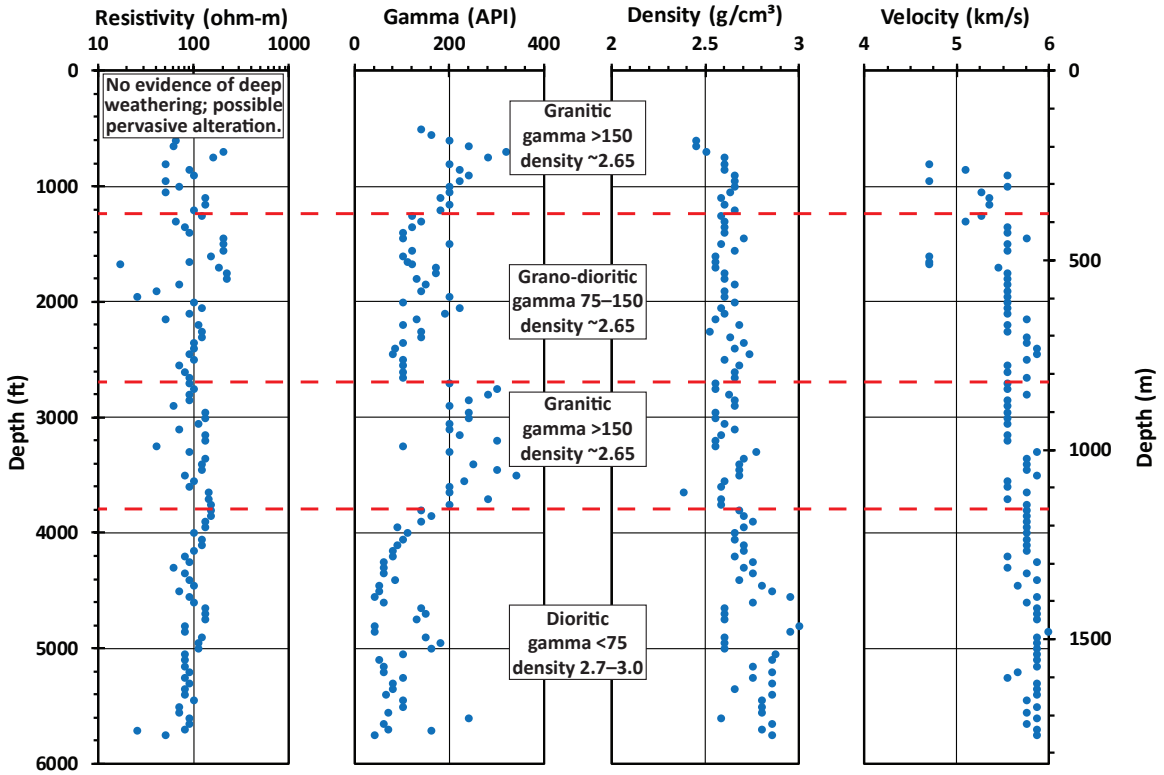

Figure 8. *Smoothed resistivity, gamma, density, and velocity log responses from well 82-33 located about 1.6 miles northeast of the 58-32 well. The well penetrated granite, granodiorite, and diorite that, outside of various analyses of cuttings or core, can typically be best identified by density and gamma logs.*

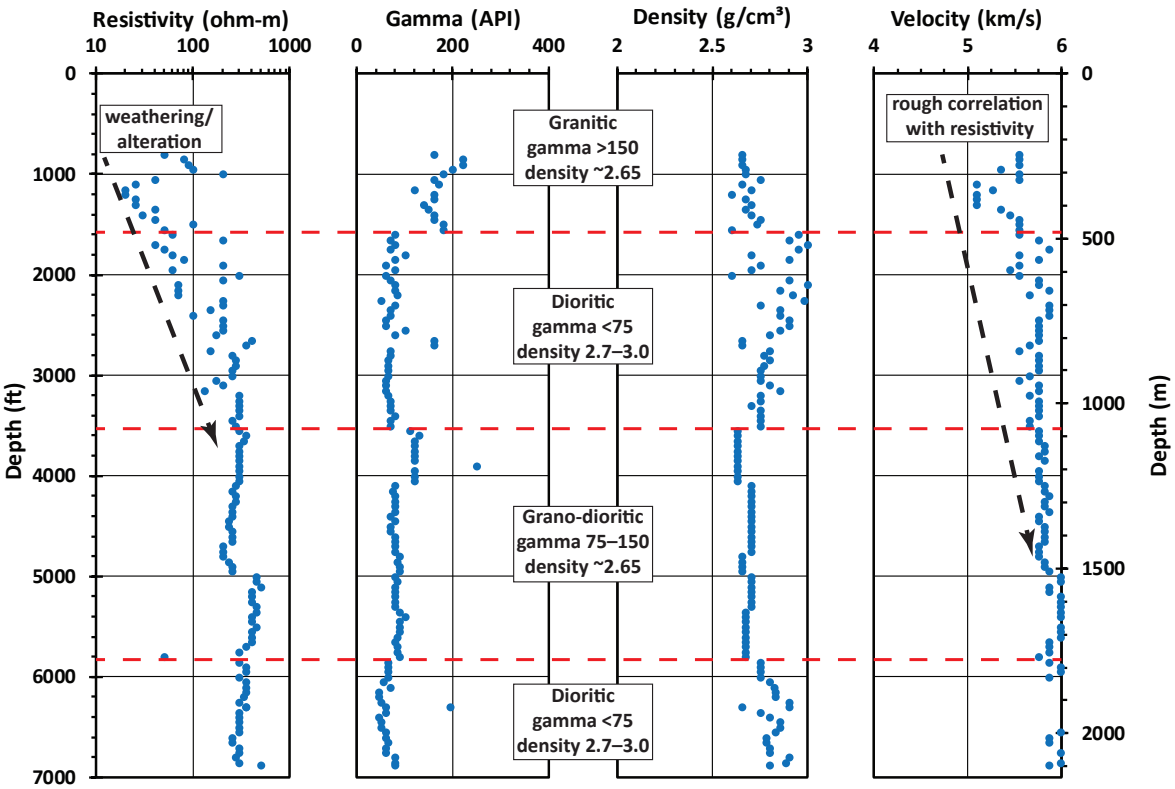

Figure 9. *Smoothed resistivity, gamma, density, and velocity log responses from well 9-1 located about 1.6 miles southeast of the 58-32 well. The well penetrated granite, granodiorite, and diorite that, outside of various analyses of cuttings or core, can typically be best identified by density and gamma logs.*

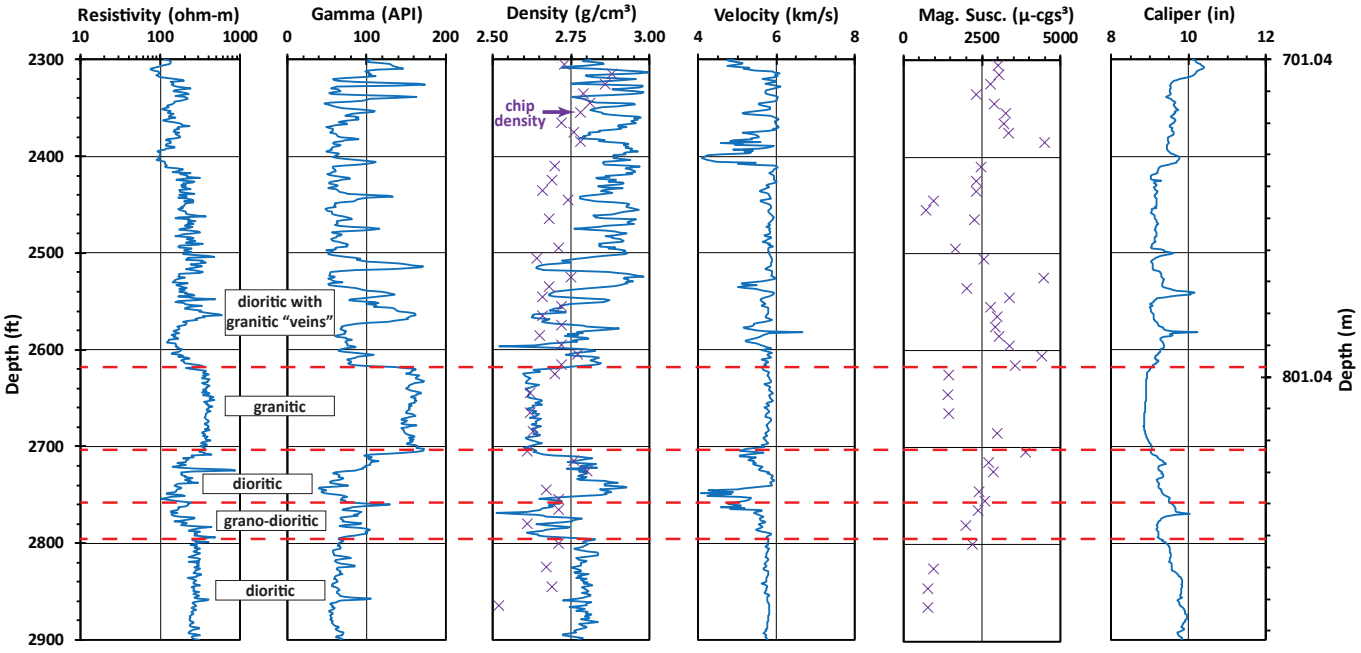

Figure 10. *Smoothed caliper, resistivity, gamma, density (logged and calculated from drill cuttings), sonic, and magnetic susceptibility (from cuttings) responses from a 600-foot section of well 9-1 (subset of "dioritic" interval on Figure 9). While this interval is located within a diorite zone, smaller veins and larger intervals of more granitic or granodioritic (intermediate) compositions are present. Increased magnetic susceptibility is generally correlative with more mafic (dioritic) compositions as these contain more iron-rich minerals.*

Figure 11. *Small-scale intrusions of lighter-colored granite and darker-colored diorite in an outcrop about 2.4 miles northeast of well 58-32. Similar small-scale lithologic variations can be seen at many other outcrop locations in the Mineral Mountains east of the FORGE site.*

The purpose of the first four runs (Figure 12) was to study the thermal recovery of the borehole to estimate the in situ formation temperature. This was necessary due to the thermal disturbance caused by drilling, particularly the circulation of relatively cool drilling fluids. Numerous studies have investigated the thermal effects of drilling, and some examples include Henrikson and Chapman (2002), Ascencio and others (2006), Goutorbe and others (2007), Edwards and Chapman (2013), and Gwynn and others (2014). Because the DOE requirements for FORGE specify a minimum resevoir temperature of 175°C (347°F) at 2 kilometers depth (6560 feet), it was important to estimate the equilibrium temperature at this depth (6800 feet) to ensure that suitable temperatures would exist at the final planned TD. Analysis of the temperature data from the 6800-foot runs suggested an equilbrium temperature of 181°C (358°F). The fifth run was accomplished after the wellbore was static for 37 days, allowing for a return to near-thermal equilibrium. The sixth, and final, temperature log was run after the well was static for over one year (408 days) to assess the undisturbed formation temperature. These logging runs confirm temperatures are suitable for the FORGE project (180°C at 2.0 kilometers and 199°C at the TD of 2.3 kilometers). Additional information on the thermal regime of the FORGE area is in Allis and others (2018a, 2018b).

Geophysical and Image Logging

Schlumberger wireline logs were run in the open-hole section of the well from the bottom of the 9-5/8-inch casing at 2173 feet to the total depth of 7536 feet on September 15, 2017. These logs included a FMI (image) log. A cement bond log was run on September 19–20, 2017, to assess the quality of the cementation of all the casing in the well. A second FMI run was made on September 24, 2017, to assess formation changes following a Diagnostic Fracture Injection Test (DFIT) in the open-hole segment below the 7-inch casing (see Nadimi and others, 2018). Figure 13 shows a selection of the wireline logs and the interpreted gross lithology from x-ray diffraction (XRD) data (Jones and others, 2018, 2019).

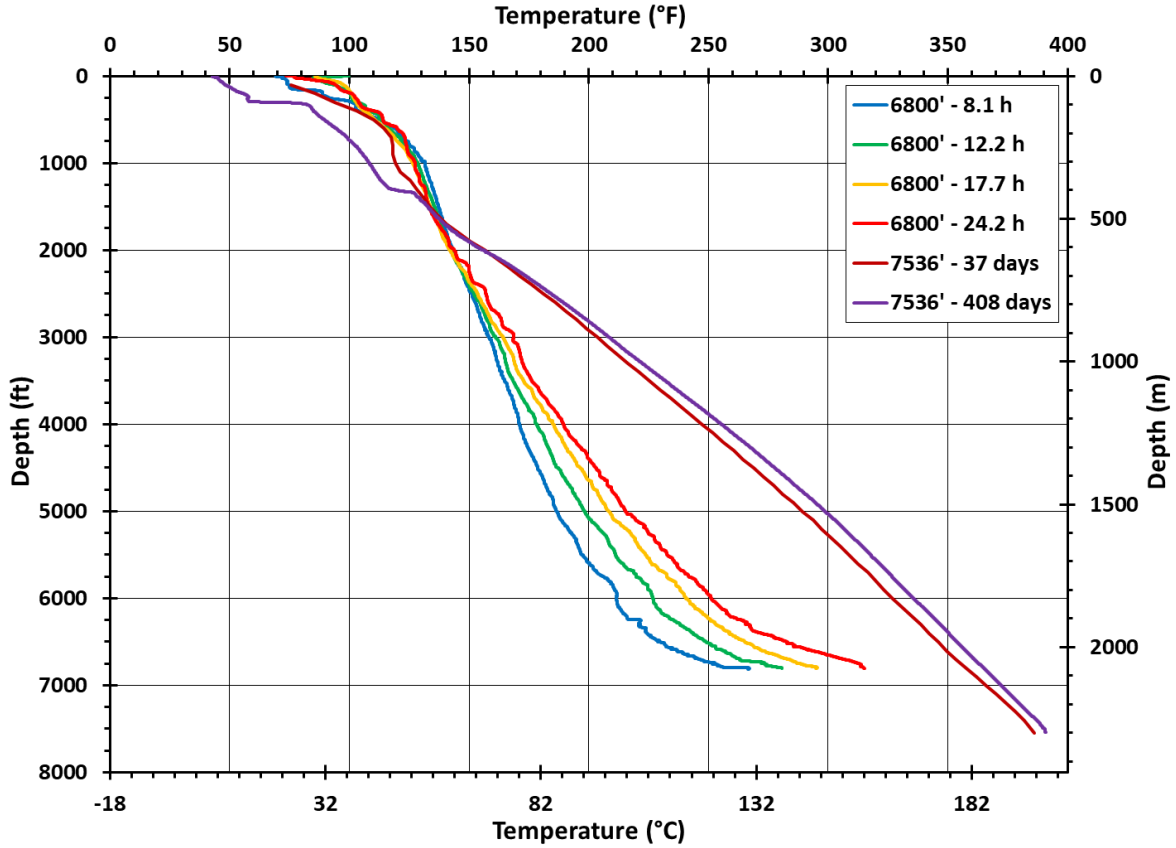

Figure 12. *Temperature-depth profiles from the four logging runs made while the bottom of the hole was at 6800 feet (September 3–4, 2017) and two additional runs to the final TD of 7536 feet (November 2, 2017 and November 8, 2018). The 6800-foot data were used to estimate an equilibrium temperature of 358°F (181°C) at this depth. The two runs to the final TD were made to obtain an initial assessment of the formation temperature after much of the drilling disturbance had been attenuated and then to determine the undisturbed formation temperature after the well had fully recovered. The final temperature at TD is 376 °F (191°C), well into the DOE-specified temperature-depth window. Cooler temperatures above 1300 feet shown in the 408-day log likely reflect groundwater flow.*

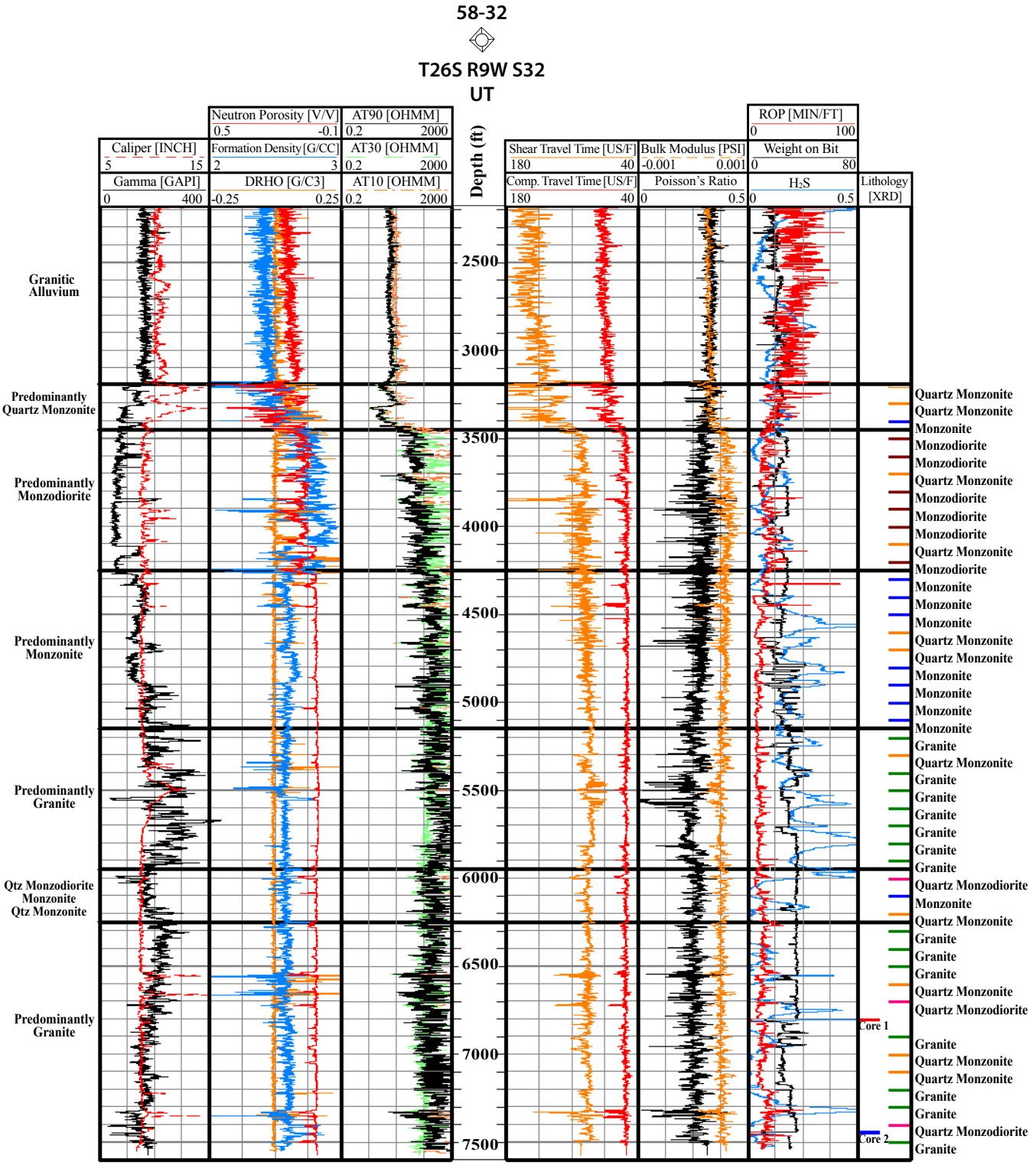

Figure 13. *Selection of wireline log responses for well 58-32 from the bottom of the surface casing at 2173 feet to TD. "Caliper" indicates hole diameter, "Gamma" indicates natural gamma radiation, "Neutron Porosity" indicates rock porosity, "Formation Density" indicates rock density, "DRHO" indicates the quality of the density data, "AT__" indicates rock resistivity, "Shear/Comp Travel Time " and "Poisson's Ratio" indicate sonic properties of the formation, "Bulk Modulus" is a measure of volumetric elasticity of the rock (a deformational characteristic), "ROP" and "Weight on Bit" indicate drilling parameters, and "H2S" is a measurement of hydrogen sulfide gas released from the formation while drilling. Rock-type "tops" on the left of the figure are defined primarily by XRD data (Jones and others, 2018, 2019) shown on the right. The gamma and formation density curves are the most useful for identifying intrusive igneous rock types. High gamma/low density responses are characteristic of granitic rocks while low gamma/high density responses are characteristic of dioritic rocks.*

FORGE 58-32 DRILL CUTTINGS AND CORE

Drill cuttings were collected at 10-foot intervals from 100 to 7500 feet (except for 6800 feet where the first core segment was obtained) by mud loggers from West Coast Geologic. Drilling fluids were rinsed from the samples, which were then bagged and dried. Two sets of samples were prepared; one set was sent to the Energy & Geoscience Institute at the University of Utah (EGI) and the other to the Utah Geological Survey (UGS). Thermal conductivity, density, spectral gamma, magnetic susceptibility, XRD, and optical analyses were performed on the samples at 100-foot intervals and some intermediate depths. Additional analyses were performed on core samples from 6800–6810.5 feet and 7440–7452 feet. Rock types determined from XRD and optical analyses are considered "ground truth" for this report and are shown or referenced in many figures herein.

Thermal Properties

Future modeling of the thermal-mechanical-fluid flow characteristics beneath the FORGE site will require knowledge of the thermal properties of the granitic host rock. Thermal properties such as thermal conductivity, specific heat, thermal diffusivity, and heat generation require laboratory measurements. Such measurements were performed on the core and selected cuttings recovered from the 58-32 well. Selected samples of outcropping bedrock from the adjacent Mineral Mountains were also collected for comparison with the 58-32 samples. The outcrop samples spanned a range of rock types based on the geologic maps of Sibbett and Nielson (2017) and Kirby and others (2018). X-ray diffraction analyses by Jones and others (2018, 2019) suggest some differences in rock types from those mapped by Sibbett and Nielson (2017).

Thermal Conductivity

Thermal conductivity measurements were made on the drill cuttings using divided bar-type equipment calibrated with fused quartz and water standards (see Allis and others, 2018a). The calibration checks showed that instrument accuracy was ±5%. The measurement cells were filled with the granular cuttings, then the air was removed under vacuum and the sample was saturated with water. Each cell was tested on each stack of the divided bar at least once, resulting in a minimum of two measurements per sample. The matrix thermal conductivity for the samples was then calculated after correcting for the mass of water in the measurement cells. The in situ thermal conductivity (at 25°C) was then calculated using porosity values from wireline logs (Gwynn and others, 2018). Both corrections used the geometric relationship for mixtures:

$$K_{mix} = K_1^{v1} \times K_2^{v2}$$

where: K is the thermal conductivity of the mixture and the two components, and v is the fractional volume of each component. Repeat measurements suggest that uncertainty is ±10%. Figure 14 shows the values and the differences between the matrix thermal conductivity and the corrected in situ (bulk) thermal conductivity.

Thermal conductivity was also measured on solid "pucks" cored and slabbed from the outcrop and well 58-32 core samples. The matrix density of the samples was calculated as part of the thermal conductivity measurements. Table 1 summarizes the results of the analyses on the outcrop samples.

Quartz has a relatively high thermal conductivity compared to many other silicate minerals, so plotting matrix thermal conductivity against weight percent quartz (Figure 15) reveals a linear relationship and two clusters of data. The low thermal conductivity cluster (2.1–2.6 W/m°C) occurs where quartz content is below 10% and corresponds to monzonite and monzodiorite compositions. The high thermal conductivity cluster (2.4–4.0 W/m°C) occurs where quartz content is above 13% and corresponds to more granitic compositions. The best-fit trendline through all the data extrapolates to a 100% quartz value of 7.5 W/m°C. This value is close to the 7.69 W/m°C average reported by Horai and Simmons (1969). Crystalline quartz can have a wide range of values but is often cited as ranging from 6 to 10 W/m°C, depending on crystal orientation (Birch and Clark, 1940; Robertson, 1988; Whittington and others, 2009).

The correlation between thermal conductivity and quartz content by depth and rock type is shown in Figure 16. Quartz content and thermal conductivity are relatively high (mainly around 18%–32% and 2.8–3.5 W/m·K respectively) in the alluvial section (above about 3200 feet), suggesting a granitic source. Values decrease to less than 12% quartz and thermal conductivities of less than 2.6 W/m·K in the zones characterized by more mafic rock (mainly monzodiorite). Thermal conductivity and quartz content increases again in the granite zone (19%–36% and 3.1–3.4 W/m·K), before decreasing in the (primarily) granitic-intermediate rock in the bottom section of the well.

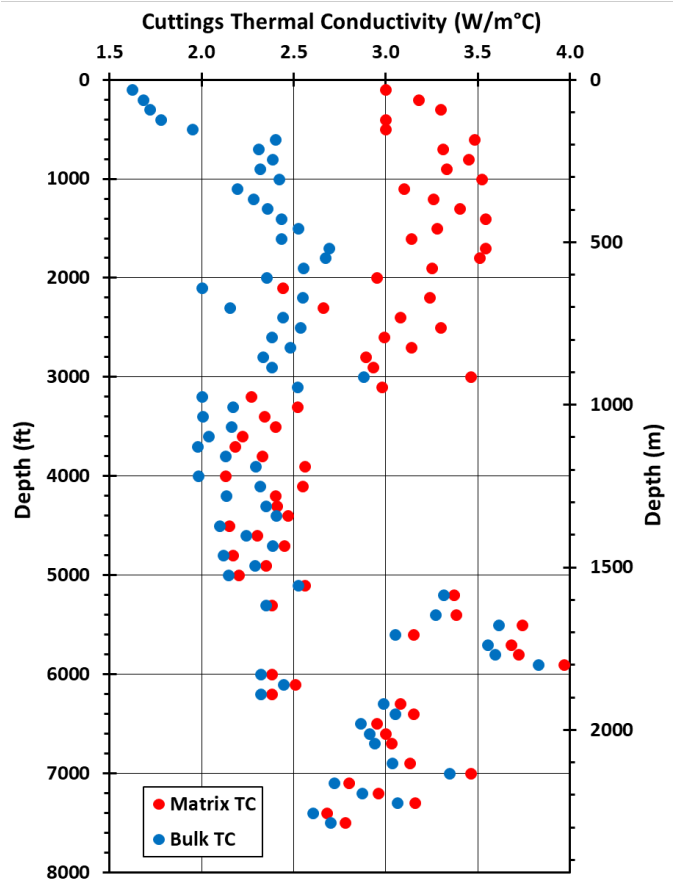

Figure 14. *Thermal conductivity data for well 58-32 based on cuttings measurements. Matrix thermal conductivity values are corrected for the effects of rock porosity using wireline geophysical logs (Gwynn and others, 2018). The variation in thermal conductivity is largely due to the quartz content of the rock. The transition from granitic basin fill to granitic bedrock occurs at about 3176 feet (Allis and others, 2018a).*

Specific Heat

Specific heat was measured with a calorimeter calibrated with water and fused quartz standards. Selected samples of cuttings and core from the 58-32 well were heated to 72°C and immersed in water at room temperature. The resulting temperature rise was measured with accuracy better than ±0.01°C. The measurement uncertainty was 0.08 kJ/kg°C, equating to about 10%. Measurements ranged between 0.7 and 1.0 kJ/kg°C. Specific heat typically increases from about 0.7 to 1.0 kJ/kg°C between 25° and 200°C (Whittington and others, 2009).

Thermal Diffusivity

Values determined from the thermal conductivity and specific heat measurements were used to calculate thermal diffusivity of the selected samples. This was done using the relationship:

$$\propto = \frac{K}{\rho \times c}$$

where: $\propto$ is the thermal diffusivity, K is thermal conductivity, ρ is density, and c is specific heat. Values range from 0.7 to 1.7 mm^2/s, with an uncertainty of 15% (measurements at 25°C). Recent measurements suggest the typical crustal rock thermal diffusivity decreases from about 1.7 to 1.0 between 25° and 200°C (Whittington and others, 2009). Table 2 summarizes the results of these analyses.

Both thermal conductivity and thermal diffusivity decrease with increasing temperature. Based on the range of measurements shown in Figures 14, 15, and 16, and measurements of eastern U.S. granites at various temperatures (Robertson, 1988), the reservoir thermal conductivity will be about 15% lower than the laboratory measurements at room temperature.

Table 1. *Thermal conductivity and density measurements on outcrop samples from the Mineral Mountains (measurements at 25°C). T, Tertiary; Q, Quaternary; gr, fine-grained granite; rf, rhyolite flow; s, syenite; qm, quartz monzonite; Xbg, Precambrian banded gneiss; gd, granodiorite; hgn, hornblende gneiss; bg, biotite granite; d, hornblende biotite diorite; hd, hornblende granodiorite.*

Sample	Mapped Unit*	Thermal Conductivity (W/m°C)	Dry Density (g/cm^3)	Saturated Density (g/cm^3)	Porosity (%)
OC1	Tgr	2.75	2.54	2.56	2
OC2	Qrf	1.32	2.05	2.14	9
OC3	Qrf	1.49	2.12	2.21	9
OC4	Ts	2.10	2.50	2.53	3
OC6A	Tqm	3.21	2.54	2.56	2
OC7A	Tgr	2.66	2.59	2.60	1
OC7B	Tgr	2.42	2.50	2.53	3
OC8	Xbg	2.38	2.62	2.64	2
OC10	gd	3.01	2.53	2.55	3
OC11	gd	2.76	2.55	2.57	2
OC12	hgn	2.16	2.63	2.65	2
OC13	Tgr	2.64	2.55	2.57	2
OC14	Tgr	2.07	2.50	2.54	4
OC15	Tbg	2.69	2.55	2.58	3
OC16	hgn	2.24	2.66	2.68	2
OC17	Xbg	2.19	2.66	2.68	2
OC18	Td	1.75	2.70	2.73	3
OC19	Tqm	2.93	2.59	2.60	1
OC20	hd	2.30	2.69	2.70	1

*Sibbett and Nielsen (2017)

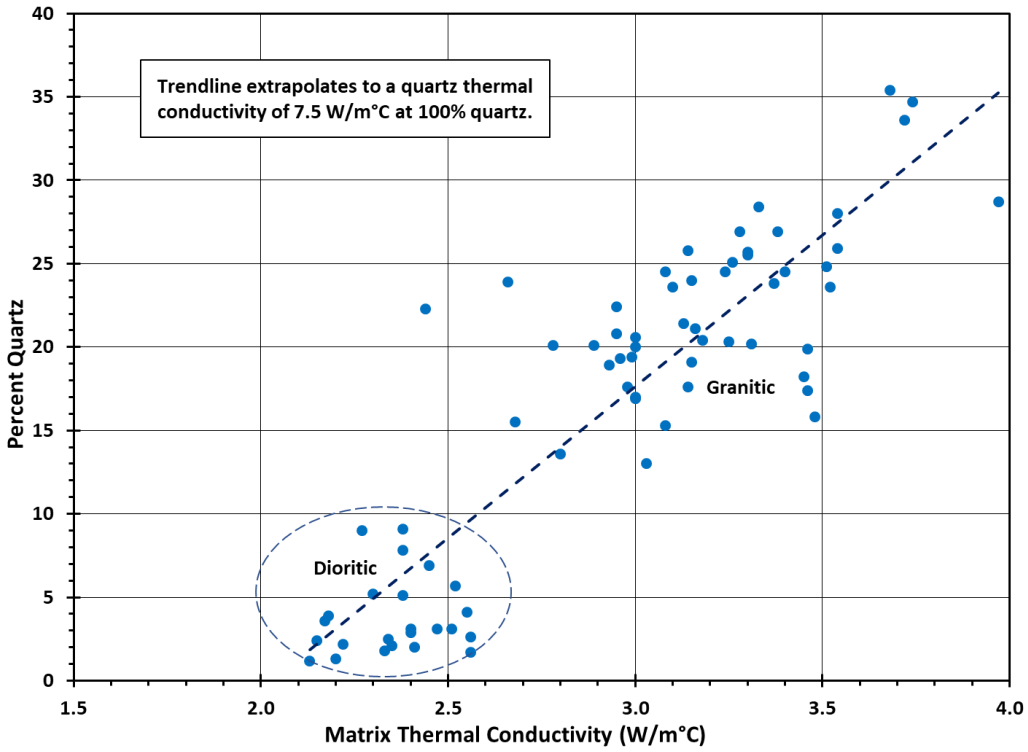

Figure 15. *Cross-plot showing the relationship between quartz content and matrix thermal conductivity in well 58-32 cuttings. The more-dioritic cuttings contain less quartz and therefore have lower thermal conductivity values than the more-granitic cuttings. The best-fit trendline projects to a thermal conductivity of 7.5 W/m°C for 100% quartz.*

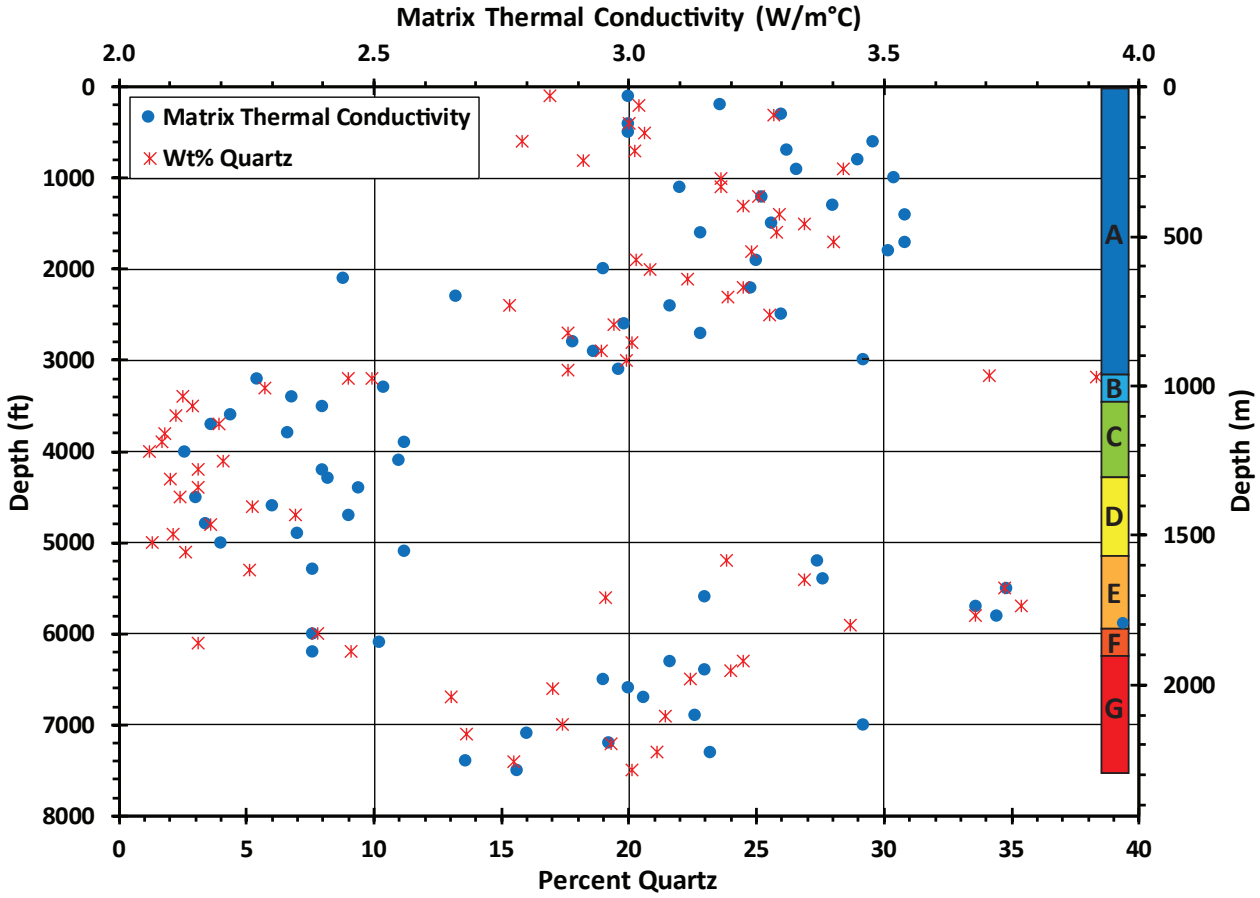

Figure 16. *Comparison of measured matrix thermal conductivity and weight percent of quartz (from cuttings at 100-foot intervals based on divided bar and XRD analyses) for well 58-32. Colored boxes on the right indicate rock types determined by XRD (Jones and others, 2018, 2019). A is mixed granitic alluvium; B is predominantly quartz monzonite; C is predominantly monzodiorite; D is predominantly monzonite; E is predominantly granite; F is a mix of quartz monzodiorite, quartz monzonite, and monzonite; G is predominantly granite with lesser amounts of quartz monzonite and quartz monzodiorite. Thermal conductivity in quartz is high compared to most minerals, so thermal conductivity is largely controlled by the quantity of quartz in these samples. The relatively high thermal conductivity and quartz content in the alluvial section (A) suggests a predominantly granitic origin. The relatively low thermal conductivity and quartz content from around 3000 to 5000 feet are typical of the monzodiorite and intermediate rock compositions through those zones. The high thermal conductivity and quartz content are consistent with the granite zone (E). Rock beneath the granite zone tends to be quartz-rich (granite, quartz monzonite, and quartz monzodiorite).*

Density

The matrix density of each sample is calculated as part of the thermal conductivity measurement and is shown in Figure 17. These data are useful for comparison with the wireline logs as well as gravity modeling (see Hardwick and others, 2018). Matrix density does not account for pore space within the in situ rock, so values need to be corrected using porosity data from other sources. The neutron porosity log for 58-32 was used for the correction below 2173 feet (bottom of surface casing/top of the log). Porosity in the deep alluvial section between the bottom of the surface casing and the top of the granitic basement at about 3300 feet shows a steady decrease from around 15% to 11% (Figure 18).

Porosity for most of this 900-foot interval varies from 6% to 9%. The rock is much tighter below 4300 feet, where porosity remains relatively constant at 1% to 2%. Because the 58-32 logs start below the surface casing, the formation density log from GPC-15 (3 miles south of 58-32) was used to calculate porosity in the shallow alluvial section. Porosity ranges from about 15% to 40% in the upper part of the alluvial section (decreasing with depth due to compaction). The bottom of the GPC-15 porosity data agrees well with the top of the 58-32 neutron porosity data. The higher porosity values cause the calculated bulk density to differ significantly from the measured matrix density in roughly the upper half of the well (alluvial and upper basement sections) compared to the low-porosity zones below. The bulk density of our granite cuttings (2.67 ± 0.08 g/cm^3) is 0.05 g/cm^3 higher than the formation density log values in granite (2.62 ± 0.08 g/cm^3).

Table 2. *Thermal properties from core and cuttings from 58-32. Measurements were made at 25°C. Thermal diffusivity was calculated from the other measured thermal properties.*

Depth (ft)	Thermal Conductivity (W/m°C)	Dry Density (g/cm^3)	Specific Heat (kJ/kg°C)	Thermal Diffusivity (mm^2/s)
Cuttings 3900	2.56	2.95	0.82	1.1
Cuttings 4500	2.15	2.71	0.79	1.0
Cuttings 7000	3.46	2.76	0.73	1.7
Cuttings 7300	3.16	2.72	0.73	1.6
Cuttings 7400	2.68	2.68	0.70	1.4
Core 6801.3	2.69	2.64	0.95	1.1
Core 6801.9	2.50	2.64	0.81	1.2
Core 6806.6	2.88	2.63	0.79	1.4
Core 6809.0	3.13	2.61	0.78	1.5
Core 7442.6	2.57	2.79	0.86	1.1
Core 7445.4	1.81	2.85	0.87	0.7
Core 7448.2	2.69	2.63	0.85	1.2
Core 7449.4	2.76	2.63	0.88	1.2
Average	**2.70**	**2.71**	**0.81**	**1.2**
Std. Dev.	**0.43**	**0.10**	**0.07**	**0.3**

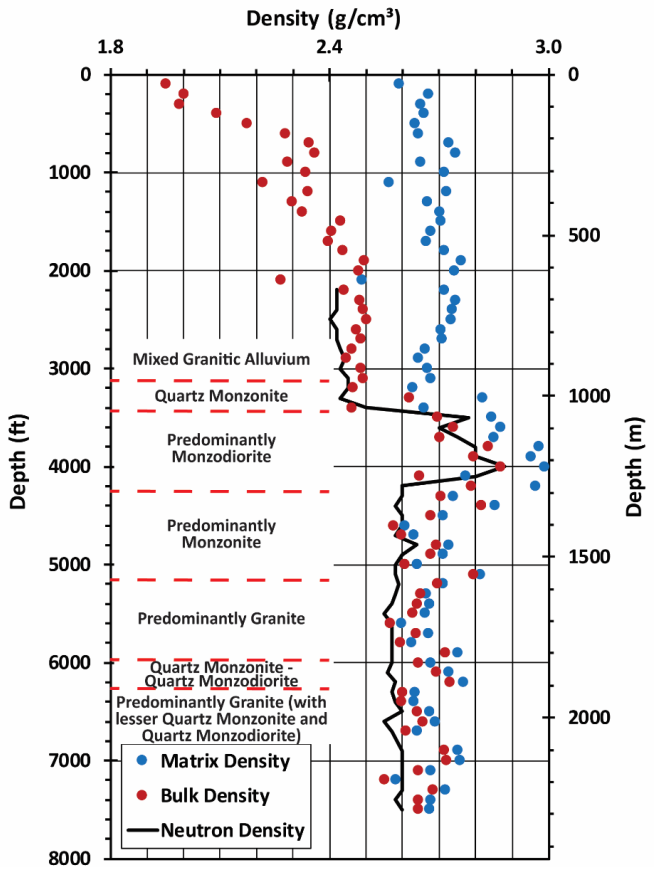

Figure 17. *Measured density values from drill cuttings at 100-foot intervals in well 58-32. Measurements taken as part of the thermal conductivity analyses yield matrix density values that must be adjusted for porosity to determine bulk density values. These measurements compare well with the wireline neutron density data starting at 2173 feet (bottom of the surface casing). Mafic minerals are the primary cause for density changes as shown by the dramatic increase between about 3500 and 4200 feet, which XRD data suggest are primarily monzodiorite. For cuttings in granite, the average bulk density is 2.67 ± 0.08 g/cm³, about 0.05 g/cm³ higher than the formation density log values in the granite zone (2.62 ± 0.08 g/cm³).*

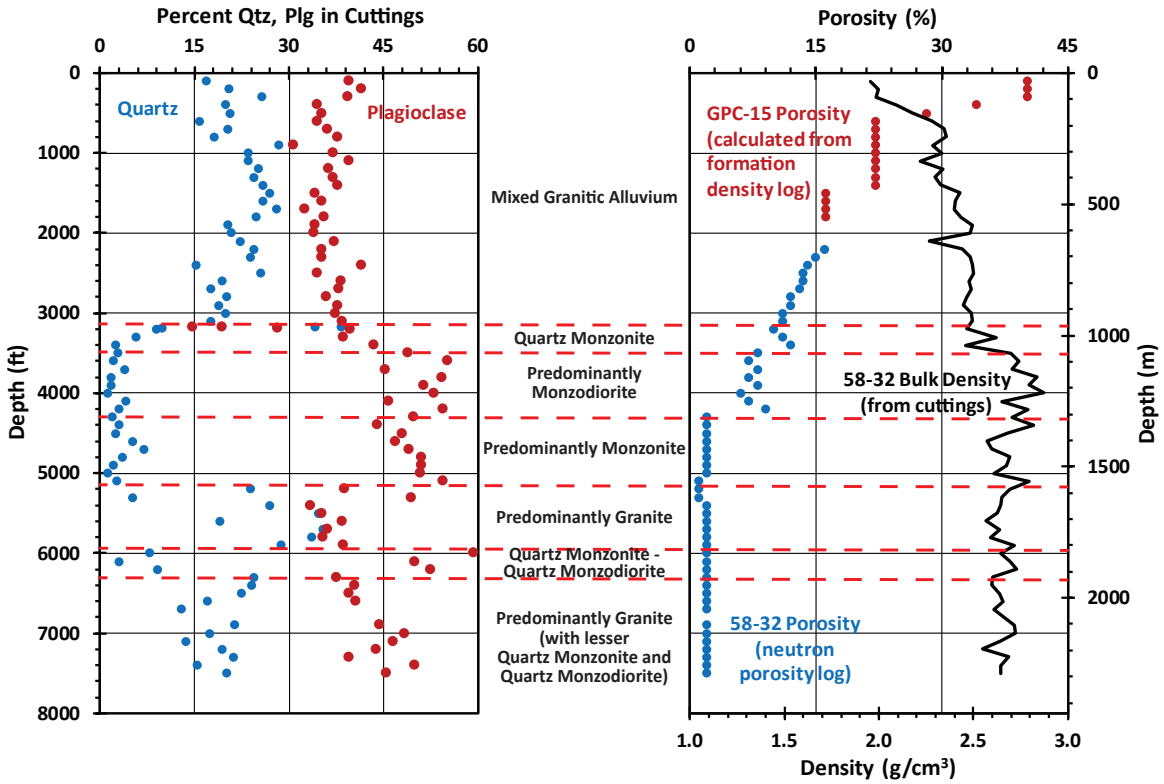

Figure 18. *Quartz and plagioclase in drill cuttings at 100-foot intervals show an inverse relationship, with low quartz and high plagioclase being diagnostic of more dioritic rock types (plot on left). The plot on the right shows porosity data (formation density logs from GPC-15 for the alluvium values above the level of the 58-32 casing, about 3 miles to the south) and well 58-32 neutron porosity log data that were used to determine bulk density from measured matrix density data. Note decreasing porosity with depth through the alluvial section, the very uniform and minimal porosity deeper in the granitic basement, and the high densities characteristic of the more dioritic zones. Except for "mixed granitic alluvium," all other rock types were determined from XRD analyses (Jones and others, 2018, 2019).*

Density changes in the well primarily correlate to compositional changes in the rock. For example, low quartz and high plagioclase in the zone characterized by monzodiorite is, to a degree, reflected by higher matrix densities as shown in Figure 19. Increasing concentrations of mafic minerals such as biotite, hornblende, titanite, apatite, and clinopyroxenes result in higher densities. Figure 19 shows that the matrix densities of granite and more-intermediate compositions typically vary between 2.58 and 2.82 g/cm^3 and have mafic compositions of less than 7% (by weight). In contrast, dioritic densities approach 3.0 g/cm^3, with mafic components ranging from about 12% to 34%. A linear correlation suggests that an ultramafic rock would have a matrix density of about 3.52 g/cm^3, and a complete lack of mafic minerals would yield a density of about 2.67 g/cm^3.

By using XRD as "ground truth" data with respect to rock types encountered in well 58-32 and comparing these data to density and other types of data, a general picture of what rock type causes a given response in the gamma and formation logs was developed. By comparing gamma and formation density logs (with the responses averaged over the same 10-foot intervals that were used for the various analyses performed on the cuttings, but only below 2200 feet where the logs start), a general identification trend develops (Figure 20). In general, density values (from formation density logs or bulk density from cuttings) below 2.5 g/cm^3 are almost certainly from alluvial sections, although the gamma values could shift depending on the source lithology (e.g., more dioritic parent rocks may produce alluvium with lower gamma signatures). Diorite (and monzodiorite) also have distinct gamma and density signatures (low gamma, high density) as do end-member granites (high gamma, low density). The intermediate rock can be reasonably discerned from the dioritic rock, but overlaps in both density and gamma with more intermediate granite. Identifying individual intermediate rock types is more challenging because gamma and density signatures for each type are less distinct and tend to overlap with one another. These characteristics can be applied to interpretations of log data for other wells in the FORGE area, but may be less diagnostic in other intrusive settings.

The XRD data show that most of the potassium content in well 58-32 is contained within potassium feldspar. Therefore, in a relative sense, potassium feldspar content reflects the potassium component of natural gamma radiation (Figure 21). This means that dioritic rocks, which are low in potassium feldspar, should have a lower gamma signal. Other data sources show this

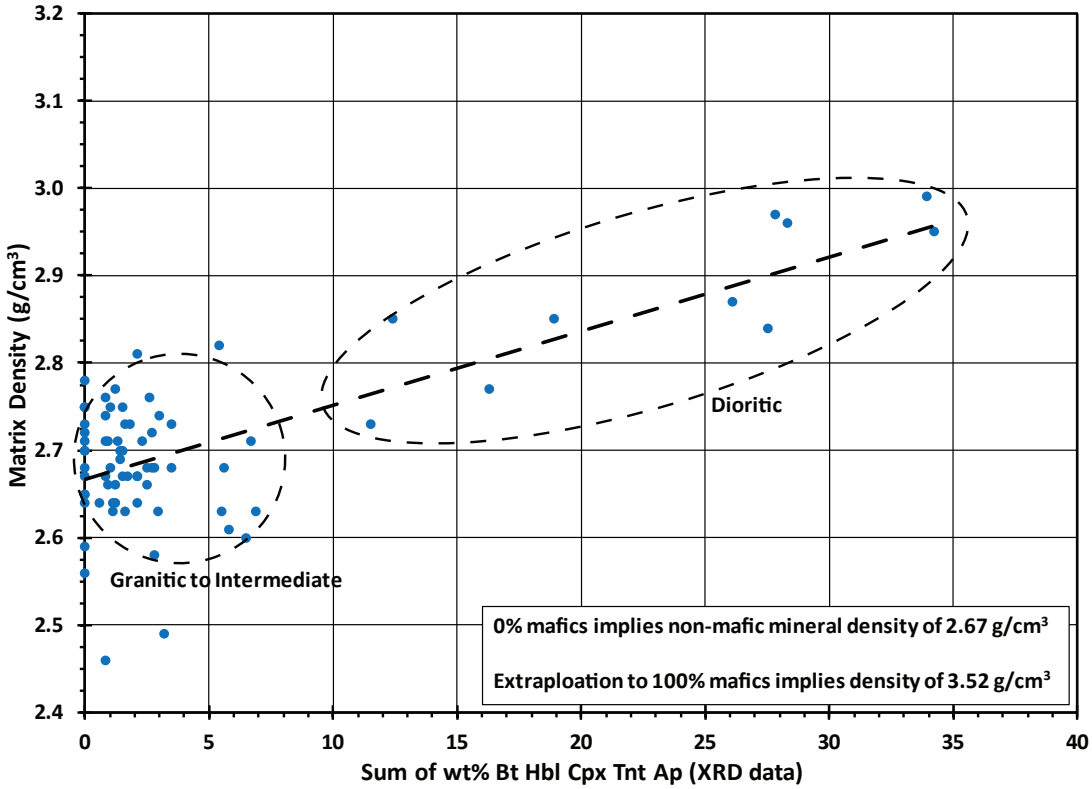

Figure 19. *Cross-plot of matrix density values and the sum weight percent of mafic minerals (biotite, Bt; hornblende, Hbl; clinopyroxene, Cpx; titanite, Tnt; and apatite, Ap) determined from XRD analyses of drill cuttings at 100-foot intervals from well 58-32 (Jones and others, 2018, 2019). The granite and more intermediate-composition rock have matrix density values of around 2.7 g/cm³ compared to more mafic (dioritic) rocks that approach 3.0 g/cm³. Extrapolation to 0% mafic minerals implies a density of about 2.67 g/cm³, compared to a 100% mafic composition where density should be about 3.52 g/cm³.*

to be true, but a quantitative value cannot be directly derived from potassium feldspar content. Potassium feldspar content in the other rock types found in the well overlap significantly and cannot be related to the total gamma signal due to the uranium and thorium components (e.g., the gamma signal is typically higher in granite than monzonite or quartz monzonite, but potassium feldspar content is generally less in granite; Figure 21). However, the same basic relationship between rock types along the x-axis in Figure 21 is present in spectral gamma plots of potassium, so there is a general relationship.

Gamma Ray Spectrometry

A Radiation Solutions, Inc. RS-230 spectrometer (Figures 22 and 23) was used to measure emitted gamma radiation from minerals containing potassium (K), uranium (U), and thorium (Th) in recovered 58-32 cuttings and core. The hand-held instrument uses a 103 cm^3 bismuth-germanium-oxide (BGO) detector. The characteristics of BGO detectors, particularly the high density (7.13 g/cm^3) and high atomic number (bismuth; 83), make the crystals very efficient gamma-ray absorbers that provide performance similar to commonly used and much larger (344 cm^3) sodium-iodide detectors (Saint-Gobain, 2016; Radiation Solutions, 2015).

Radioactive phenomena are discrete and random in nature, so statistical counting is an important part of their measurement (Blum, 1997). Therefore, accuracy and data quality are dependent on measurement duration. Three-minute assays were used to provide a good balance between data quality and measurement time, although Radiation Solutions (2015) considers two-minute assays to provide high-quality data under most conditions.

The wireline gamma logs for 58-32 are considered to be "ground truth," but they only record total gamma rather than the proportions from K, U, and Th. The spectral components, especially K, can be diagnostic of mineral composition (and therefore rock type), so spectral gamma measurements were made to complement the wireline data. Gamma radiation from the core and cuttings at a given depth should not be expected to equal the gamma values from wireline logs at the same depth. However, the relative trends should be similar, and generally are, in well 58-32.

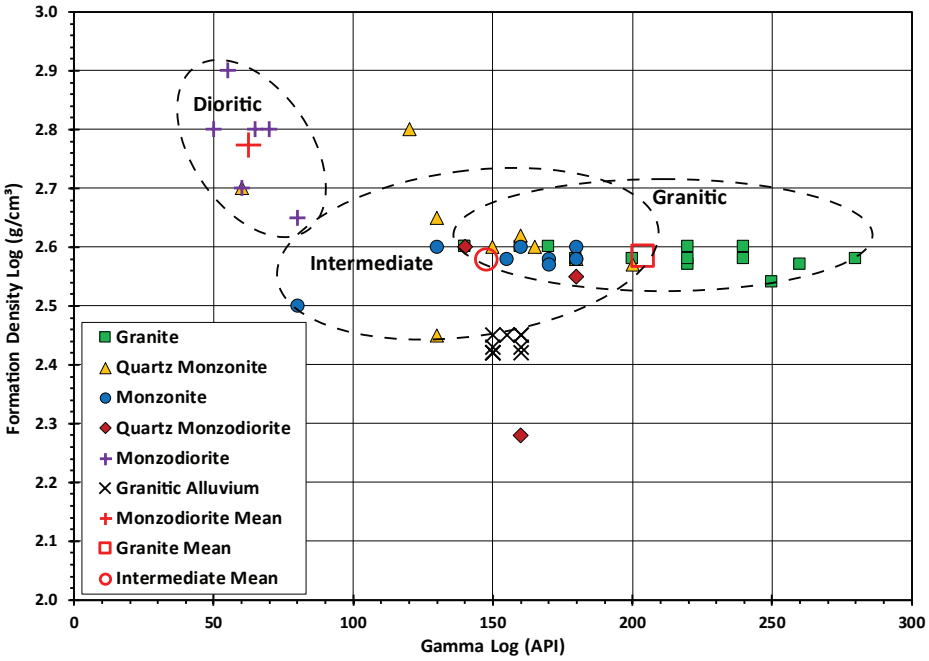

Figure 20. *Rock types and associated geophysical characteristics from log data in well 58-32. Wireline log data were analyzed at 100-foot intervals within the lower part of the alluvial section and the rest of the wellbore. Potentially faulty data due to wellbore washouts were eliminated. Data are from most of the same 100-foot intervals used for analyses on the well cuttings, but only from below 2200 feet (top of the logged section). Dioritic (diorite and monzodiorite) rock can generally be discerned by density values greater than about 2.66 g/cm³ and gamma values of 50–80 gAPI (mean is 2.77 g/cm³ and 63 gAPI). Intermediate rock (quartz monzonite, monzonite, and quartz monzodiorite) and granite generally can be discerned from dioritic rocks, but have a large degree of overlap in density and gamma values. The mean density and gamma values for the intermediate types are 2.58 g/cm³ and 148 gAPI, compared to the mean values for granite of 2.58 g/cm³ and 204 gAPI. Density values below about 2.5 g/cm³ are almost certain to be alluvial in nature, but gamma values could vary greatly depending on parent rocks. Note that bulk density values measured in the laboratory tend to be about 0.05 g/cm³ higher than formation density values from logs, and the ellipses account for slightly greater possible density values.*

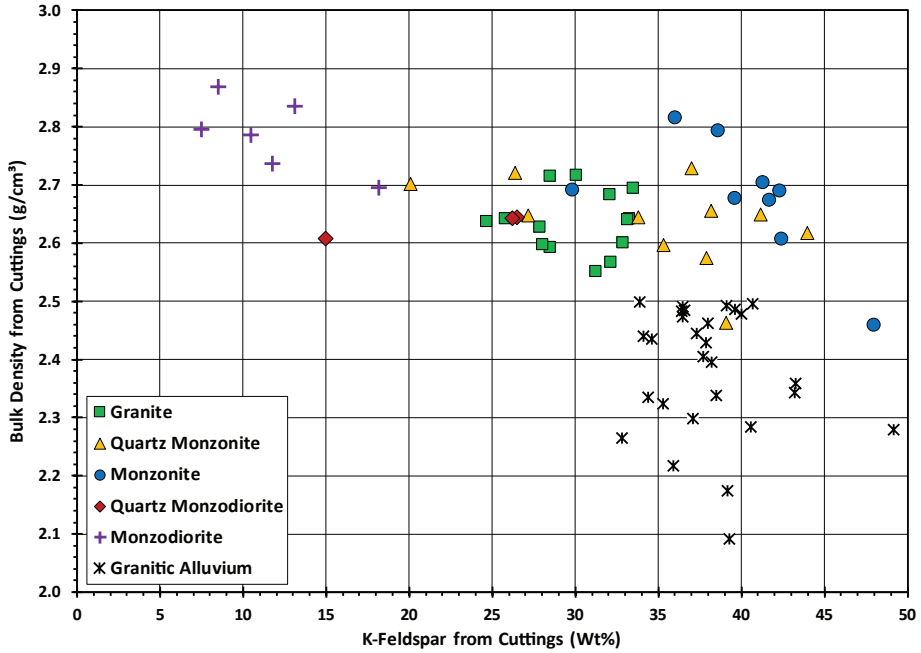

Figure 21. *Rock types from well 58-32 cuttings in terms of potassium feldspar content and measured/calculated bulk density values. Potassium feldspar content (Jones and others, 2018, 2019) and bulk density were derived from cuttings at 100-foot intervals throughout the entire well. These data were then correlated to XRD-derived rock types. Dioritic (all monzodiorite in this case) samples have distinctively low potassium feldspar composition and high density. Potassium feldspar and density values are scattered for the granitic and intermediate (quartz monzonite, monzonite, and quartz monzodiorite) rock types. Lab-measured density values for these rock types vary more than those measured by wireline logs. Density for the granitic alluvium is universally low (below about 2.5 g/cm³).*

Figure 22. *The RS-230 Gamma Ray Spectrometer in use on cuttings from well 58-32. Spectral gamma ray measurements were focused at 100-foot intervals, but due to limited sample mass, additional samples from above and below the target depth were needed to achieve a minimum mass experimentally determined from outcrop samples. Therefore, measurements were made using samples from an 80-foot interval with the spectrometer positioned over the targeted sample (photo on the right) so that the greater part of the gamma signal comes from the target depth. Measurements were made in a 5-mm-thick steel box (photo on the left) to attenuate a portion of the background gamma signal.*

Figure 23. *The RS-230 Gamma Ray Spectrometer (top center of photograph) in use on the lower core section (top at 7440 feet). Spectral gamma ray measurements were made at 3-inch intervals along the entire length of the reconstructed core. A second measurement was made on the opposite side of the core at each depth. The yellow instrument at the bottom of the photograph is the KT-10 Magnetic Susceptibility Meter that was used at the same measurement locations as the spectrometer.*

Uncertainty

Some variance in gamma readings was observed in the five gamma logs run in the 58-32 well. Such variance is due to logging speed (counting duration), logging tool calibration, and other factors, but the differences tend to be small. The gamma tools each recorded roughly 15,000 measurements and, while a few depths had large variations in recorded values, the average difference among all five tools at a given depth was about 21 gAPI with a standard deviation of 8.4 gAPI.

Spectral gamma measurements taken at the surface have some inherent deficiencies when compared to downhole measurements. Perhaps the most important is the presence of background atmospheric gamma radiation that is not present deep within the well bore. This effect was partially attenuated by making measurements on the cuttings in a 5-mm-thick steel box. No shielding was available for the core measurements, due to the length of many of the intact core segments.

To characterize the effect of background radiation on the cuttings and estimate the precision of the instrument, 20 measurements (3-minute assays) were made in the steel box without any samples. This testing showed K to be 0.58 ± 0.5%, U to be 1.99 ± 0.17 ppm, and Th to be 3.38 ± 0.25 ppm.

Although cuttings sample volumes collected in the 58-32 well are much larger than those commonly collected in deep wells, the initial spectral gamma ray measurements showed that the sample quantity was not sufficient to obtain reliable results. To determine how much granular material of granitic composition would be required to obtain reasonable measurements, 33 3-minute assays (three per location) were taken on a granitic outcrop sample from the Mineral Mountains. Measurements did vary between the 11 measurement locations (K: 1.4%–2.1%, U: 2.9–4.4 ppm, and Th: 8.2–13.4 ppm). The spectral components for the overall outcrop sample were: K: 1.7 ± 0.19%, U: 3.6 ± 0.41 ppm, and Th: 10.3 ± 1.1 ppm. The outcrop sample was then crushed and sieved to approximate the size of the cuttings obtained from the 58-32 well. These "pseudo cuttings" were placed in sample bags each weighing 700 grams and various combinations with respect to the number of bags (equating to the optimum sample mass) and their spatial arrangement were tested until results similar to the uncrushed rock were obtained. These results showed that an aggregate sample mass of about 5–6 kilograms, with the sample bags arranged so they create a volume of about 25x25x4 cm, provided the best results. This was used as a guideline for arranging the actual cuttings during the measurements.

Because the measurements are taken along the length of the cylindrical core with a 4-inch diameter, the flat surface of the 2.4-inch-diameter detector cannot be placed flat against the sample, leading to a decrease in detected gamma radiation (the top of the circular detector surface can be seen above the core in Figure 23). To assess this effect, about 5 kilograms of the "pseudo cuttings" were packed into a 4-inch-diameter cardboard cylinder and the gamma radiation was measured with the spectrometer. These results showed that core measurements may be decreased roughly 50%–70% due to detector-core geometry.

Measurements on cuttings

Measurements on the cuttings using 3-minute assays were performed on the same 100-foot intervals as used for other analyses (XRD, thermal conductivity, etc.), but due to limited sample mass additional samples from above and below the target interval had to be included (based on the sample mass testing described above). Available sample mass was still typically below the optimum of around 5.5 kilograms, but could not be increased without overlapping samples from one 100-foot interval to the next. The arrangement placed the samples closest to the target interval nearest to the detector, so that much of the spectral gamma signal was from close to the target interval. The results are shown in Figure 24. The relative lack of potassium, due to low quantities of potassium feldspar in the monzodiorite zone, is distinct, while the more granitic zones tend to be enriched with thorium. Total gamma was calculated from the spectral components for comparison with the wireline logs using the formula:

$$16K+8U+4Th = Total\ Gamma\ Ray\ (API)$$

where: K is potassium in percent, U is uranium in parts per million, and Th is thorium in parts per million. Figure 25 plots the calculated total gamma against wireline gamma (smoothed to the same 100-foot intervals as the cuttings). The calculated total gamma data and wireline gamma data follow the same trends; however, the calculated values are generally about one-third of the values from the wireline logs (Figures 25 and 26). This is likely due to most samples being at or below the calculated minimum mass threshold (also requiring material from above and below the target depth) and the lower density of loose cuttings compared to solid rock. Note that the intercept in Figure 26 is not at zero, which is probably an effect of background gamma and possibly some instrument bias.

While the absolute gamma values do not correlate well, the relative values appear correlative. Therefore, the ratios of spectral gamma components are likely accurate and useful to other calculations and interpretations. The large difference between the two data sets in the "C" zone (primarily monzodiorite) means that calculated and logged total gamma values are about 1:1 (i.e., about 50 gAPI). Comparing the potassium component from the spectral measurements and the total gamma from the logs against the potassium feldspar component from XRD analyses shows that there is excess scatter in the wireline total gamma log responses (due to differing ratios of K, U, and Th) compared to the reasonably linear correlation between cuttings-derived K-feldspar concentrations and spectral-gamma-measured percent K (Figure 27).

The radioactive decay of isotopes of K, U, and Th releases heat. Rocks with high concentrations of these elements can generate sufficient heat to be a significant factor augmenting surface heat flow when present in thicknesses of thousands of feet. The calculated total values from the spectral gamma measurements were scaled to match the API value for total gamma obtained at the same depth from the downhole logging, and the relative proportions of K, U, and Th were used to calculate heat generation. The resulting average for granitic rock in well 58-32 (granite, quartz monzonite, monzonite) and dioritic rock (quartz

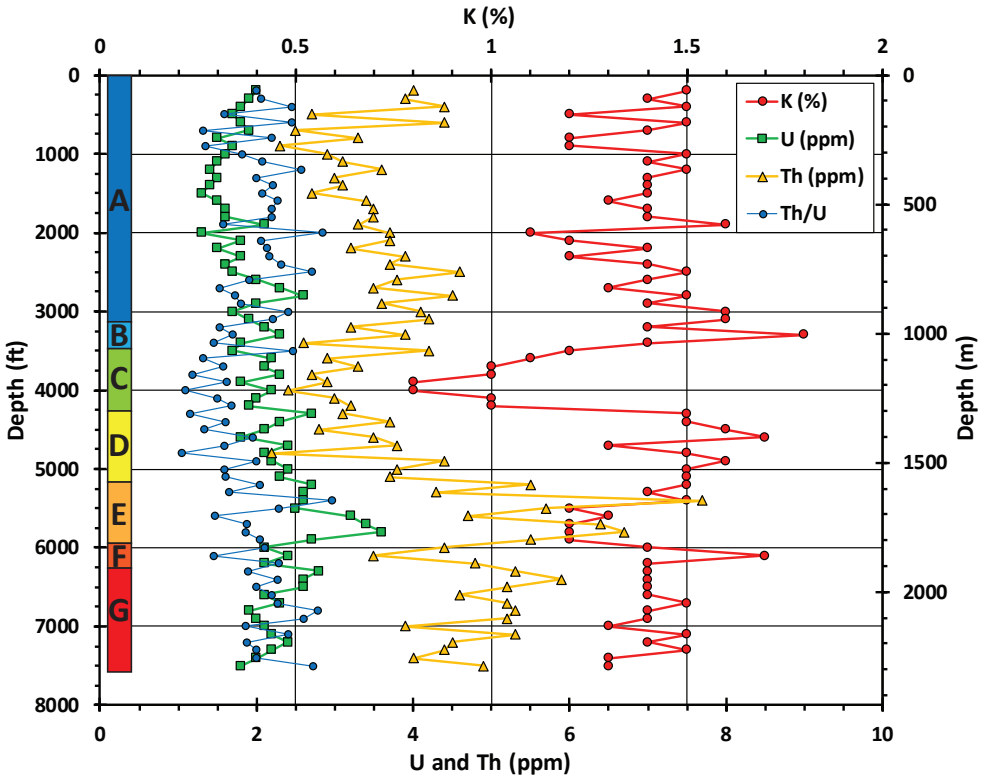

Figure 24. *Spectral gamma ray data from well 58-32 cuttings at 100-foot intervals. The spectrometer records the potassium (K) component as a percent, while uranium (U) and thorium (Th) components are recorded as parts per million (ppm). Due to limited sample mass of the cuttings at the test intervals, most measurements were made using samples from an 80-foot interval with the spectrometer positioned over the targeted sample so that the greater part of the gamma signal comes from the desired depth. Colored boxes on the left indicate rock types determined by XRD: A is mixed granitic alluvium; B is predominantly quartz monzonite; C is predominantly monzodiorite; D is predominantly monzonite; E is predominantly granite; F is quartz monzodiorite, quartz monzonite, and monzonite; G is predominantly granite with lesser amounts of quartz monzonite and quartz monzodiorite. Low K values correlate to decreased potassium feldspar (and increasing mafic minerals) in the zone that is mainly characterized as monzodiorite (about 3450–4250 feet). The more granitic zones (about 5250–5950 feet, and, to a lesser extent, 6250 feet to TD) show low to moderate K concentrations, but are relatively enriched in Th (primarily) and U (secondarily). Therefore, total gamma responses for the granitic zones are higher than for the other zones.*

monzodiorite and diorite) are shown in Table 3. A heat generation of 2–3 μW/m^3 is typical for granitic rock, but its effect on the geotherm in the upper crust is negligible because of the relatively high conductive heat flow at this site (the effect is a 2°C decrease in temperature over 5 km).

Measurements on cores

Two measurements were made at 3-inch intervals along the reconstructed length of the core, with the measurements made on opposite sides of the core (Figure 23). The measurement locations were picked to avoid fractures (natural and induced) or missing pieces of the core so that the maximum volume of rock would be adjacent to the spectrometer. Measurements on or near fractures were less reliable than those made in more competent sections of the core. These measurements show that compositional changes occur over small intervals in depth (feet or less). Distinct examples are at about 6805.5 feet in Figure 28 and in the felsic banding at about 7441.5 feet in Figure 29. This variation is not unlike that in the granitic outcrop sample used to generate the "pseudo cuttings." The differences between the calculated total gamma and the wireline gamma logs are smaller than with the cuttings samples, but the calculated values are still around 50% that of the wireline values. Like the cuttings, though, the total gamma values in the more dioritic core sections are much closer to the down-hole log readings.

Magnetic Susceptibility

A Terraplus Inc. KT-10 Magnetic Susceptibility and Conductivity meter was used to measure the magnetic susceptibility (MS) of both core sections and the cuttings from well 58-32 (Figure 23). Increases in magnetic susceptibility are due to increasing quantities of iron-bearing minerals, which in this case are mafic minerals indicative of more dioritic rock compositions.

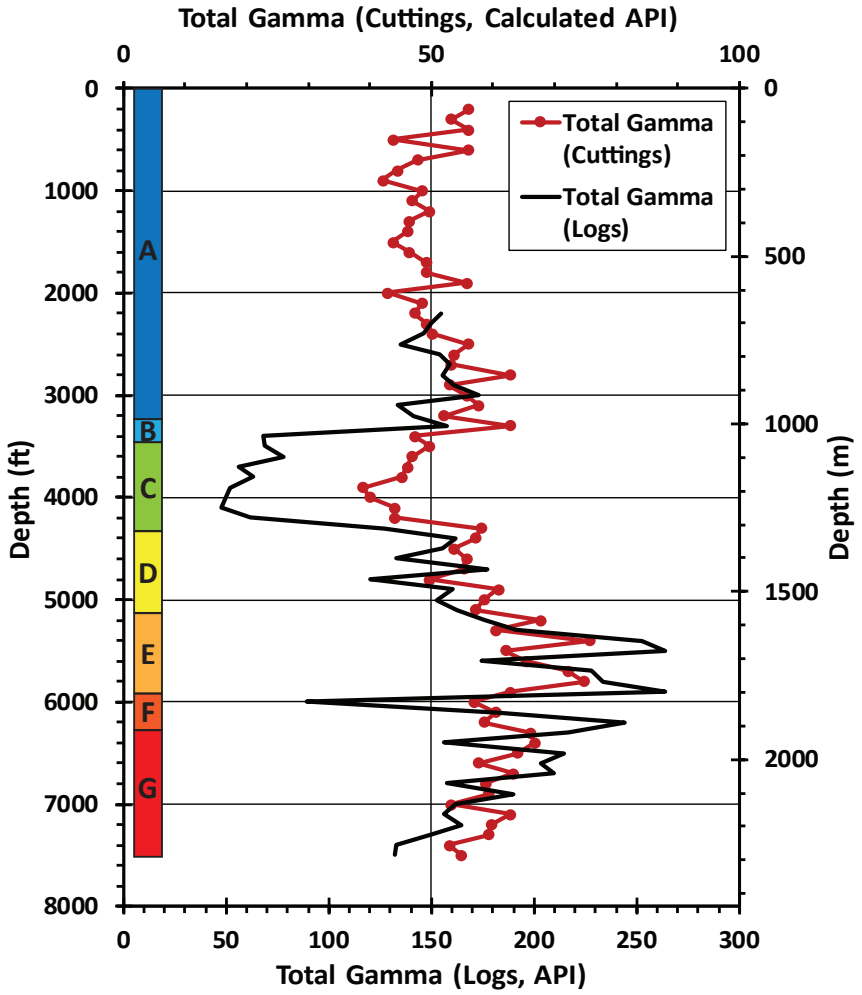

Figure 25. *Comparison of smoothed (data at 100-foot intervals) wireline gamma log and total gamma measurements (from the same intervals) for well 58-32. Measurements on the cuttings are spectral gamma (broken into contributions of potassium, uranium, and thorium), but were converted to total gamma. The wireline logs were run from 2173 feet (just below surface casing) to TD at 7536 feet. Due to limited sample mass of the cuttings at the sampled intervals, measurements were made using samples from 80-foot intervals with the spectrometer positioned over the targeted sample so that the greater part of the gamma signal comes from the desired depth. Colored boxes on the left indicate rock types determined by XRD: A is mixed granitic alluvium; B is predominantly quartz monzonite; C is predominantly monzodiorite; D is predominantly monzonite; E is predominantly granite; F is quartz monzodiorite, quartz monzonite, and monzonite; G is predominantly granite with lesser amounts of quartz monzonite and quartz monzodiorite. There is reasonable agreement in all sections of the curves except for the predominantly monzodiorite zone (about 3450–4250 feet). Logged API data are generally about three times higher than the total calculated API of the cuttings.*

Uncertainty

No accuracy specifications for the meter are supplied by the company. To help constrain measurement uncertainty, 20 measurements were made at the same location on each of two outcrop samples. The first was from outcrop mapped by Sibbett and Nielsen (2017) as Tertiary granite dikes (Tgr) and the second as Tertiary diorite (Td). Jones and others (2018, 2019) used XRD to confirm the Tgr sample is granite and classify the Td sample as quartz monzonite. The Tgr MS values range from 10.2 to 10.3 SI units with a standard deviation of 0.04. The Td MS values range from 36.3 to 38.6 SI units with a standard deviation of 0.58.

The KT-10 instrument is typically used to measure magnetic susceptibility on outcrop or on core samples. The instrument can be optimized for various core diameters ranging from 1 inch to 4.7 inches (2.54–12.00 cm) and for full diameter or split core. Therefore, the instrument is ideal for measuring the 58-32 core samples.

Because the meter is not optimized for use with cuttings, an effort was made to calibrate it using the same "pseudo cuttings" used to calibrate the spectral gamma meter. Prior to crushing the outcrop sample, five magnetic susceptibility measurements were made at 12 locations on the sample. Due to the heterogeneity of granitic rocks, the average magnetic susceptibility for each location varied from 5.51 to 9.67 SI units (variability at each location was minimal), yielding a "whole rock" average of 8.32 SI units.

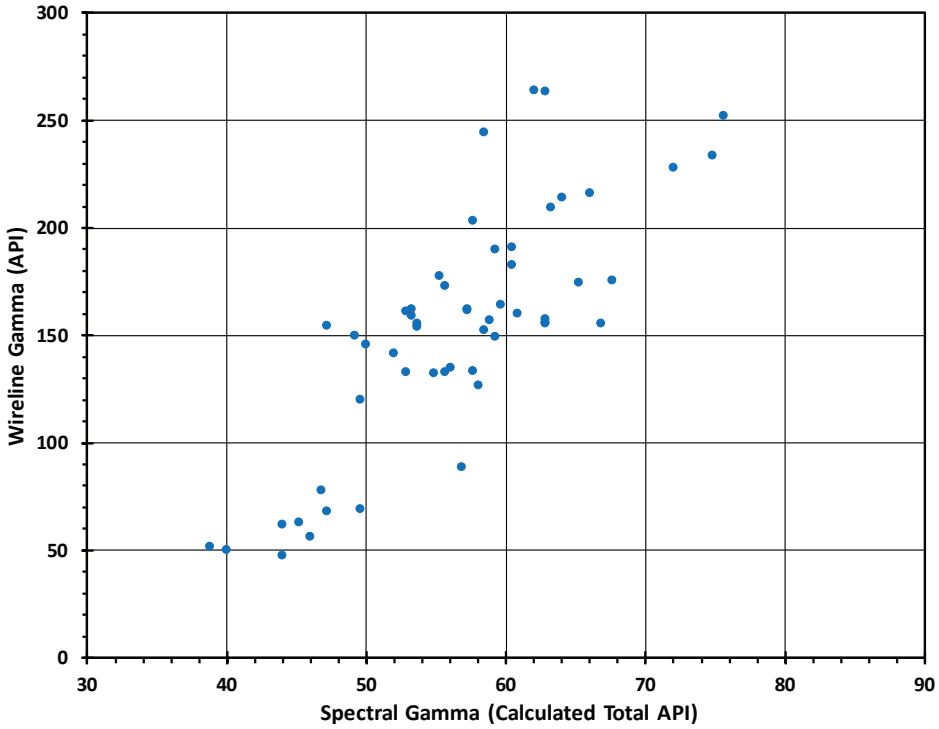

Figure 26. *Cross-plot of wireline gamma and total gamma calculated from spectral gamma data (at 100-foot intervals from 2200–7500 feet) in well 58-32. Measurements on the cuttings are spectral gamma (broken into contributions of potassium, uranium, and thorium), but were converted to total gamma. Wireline gamma values range from about 1.1 to 4.3 (2.64 average) times the calculated value from the spectral gamma measurements for a given depth. This is likely due to relatively small samples available from cuttings (2.3–5.7 kg, 4.1 kg average) despite using samples from an 80-foot interval with the spectrometer positioned over the targeted sample so that the greater part of the gamma signal came from the desired depth. A possible additional factor is that the cuttings were loosely packed in sample bags, compared to solid rock in the wellbore. However, the potassium, uranium, and thorium ratios are assumed to be reasonably accurate and useful to other analyses.*

The mass for each of the 58-32 cuttings samples (at the analyzed 100-foot intervals) varied from less than 300 to over 700 grams. Because the meter seemed to be sensitive to differences in sample mass, it was calibrated to a sample mass of 300 ± 1 grams using the "pseudo cuttings" (85% of the 58-32 samples surpassed this threshold). This was done by filling nine sample bags with 300 ± 1 grams of the "pseudo cuttings" and measuring the MS of each bagged sample five times using various meter configurations. The composite average of these measurements was then compared to the composite MS taken on the outcrop sample prior to crushing. The 2.4 inch (6.0 cm) split core configuration yielded an average magnetic susceptibility of 8.36 SI units compared to 8.32 SI units from the pre-crushed sample (measured with the meter optimized for outcrop samples). Other samples varied above and below the outcrop average by increasing magnitudes.

For cuttings samples with a mass over 300 grams, the cuttings were temporarily poured out and then 300 ± 1 grams were added back to the fabric sample bag and the MS was measured five times. For samples with less than 300 grams available, additional material from the next-deepest sample was measured along with the entire targeted sample (in separate sample bags) to create a composite sample of 300 ± 1 grams.

Measurements on cuttings

Magnetic susceptibility values generally correlate well with the XRD data from Jones and others (2018, 2019). Figure 30 compares the MS data with XRD-determined minerals that do, or may, contain iron. Comparisons were made with primary mafic minerals (biotite, hornblende, augite, titanite, and apatite) and then with the addition of other minerals that may contain iron (smectite, illite, chlorite, and epidote). Because these additional minerals are mainly found in the alluvial section, XRD differences in the granitic basement are less pronounced (MS values in the alluvial section are uniformly low). The most mafic section (predominantly monzodiorite) correlates to the highest MS values (about 18 to 47 SI units). Except for monzonite, MS values in the granitic and intermediate-composition rock fluctuate between about 2 and 10 SI units.

The measurement at 2200 feet is anomalously high and isolated compared to measurements directly above and below. The most likely explanation is that the sample is contaminated with steel particles from the drilling operation.

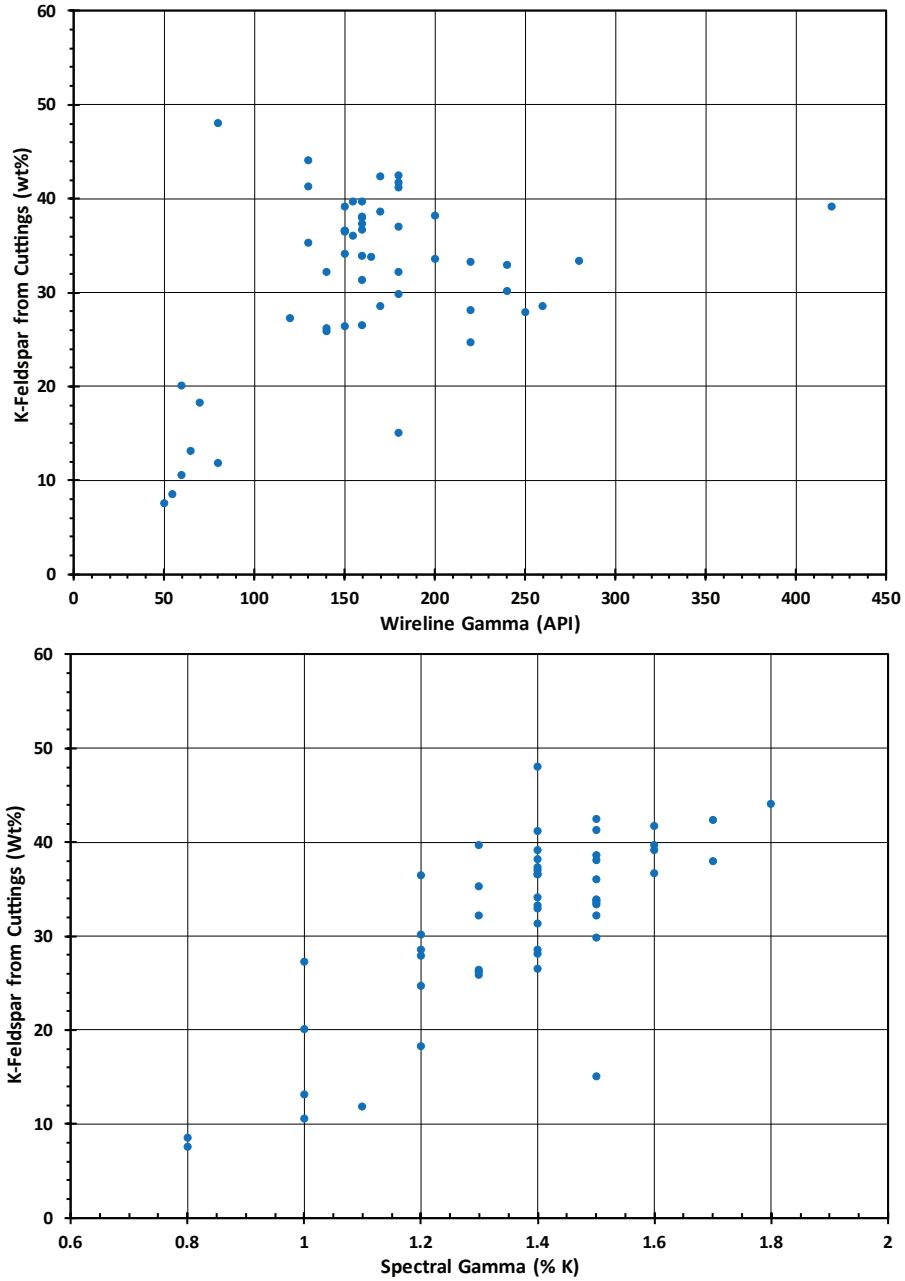

Figure 27. *Potassium component of spectral gamma data from cuttings at 100-foot intervals and total gamma from wireline logs at the same intervals (all from 2200–7500 feet) plotted against concentrations of potassium feldspar from XRD data (Jones and others, 2018, 2019). Scatter is greater with the wireline logs due to varying concentrations of thorium (primarily) and uranium. Additionally, spectral gamma data suggest thorium plays a larger role in increasing total gamma levels in granitic rock than in other rock types.*

Measurements on cores

The MS measurements were taken at the same locations as the spectral gamma measurements, with five measurements taken at each location for increased data confidence (Figures 31 and 32).

Roughly the top half of the upper core has been identified as granite-granodiorite based on XRD and petrographic analyses (Jones and others, 2018, 2019). The bottom half is granite, but closer to quartz monzonite in composition. Magnetic susceptibility in the top section ranges from near zero to about 22 SI units, whereas the bottom half is generally greater than 20 SI units. A pronounced boundary between the sections correlates with the visual and XRD-derived change in composition. The top half of the lower core has been identified as diorite, whereas the bottom half ranges from quartz monzonite to granite. Magnetic susceptibility varies widely (about 25–70 SI units) through most of the diorite, and correlates closely with several more-felsic bands within this section. The bottom half is compositionally more like the upper core and exhibits a similar range of MS values (about 20–40 SI units).

Table 3. *Heat generation characteristics of the granitic and dioritic rock encountered in well 58-32 (Allis and others 2018a).*

Rock Type	K (%)	U (ppm)	Th (ppm)	Density (kg/m3)	Heat Generation (µW/m3)
Granitic	4.0	6.7	12.4	2700	3.0
Diorotic	2.4	4.1	7.9	2800	2.0

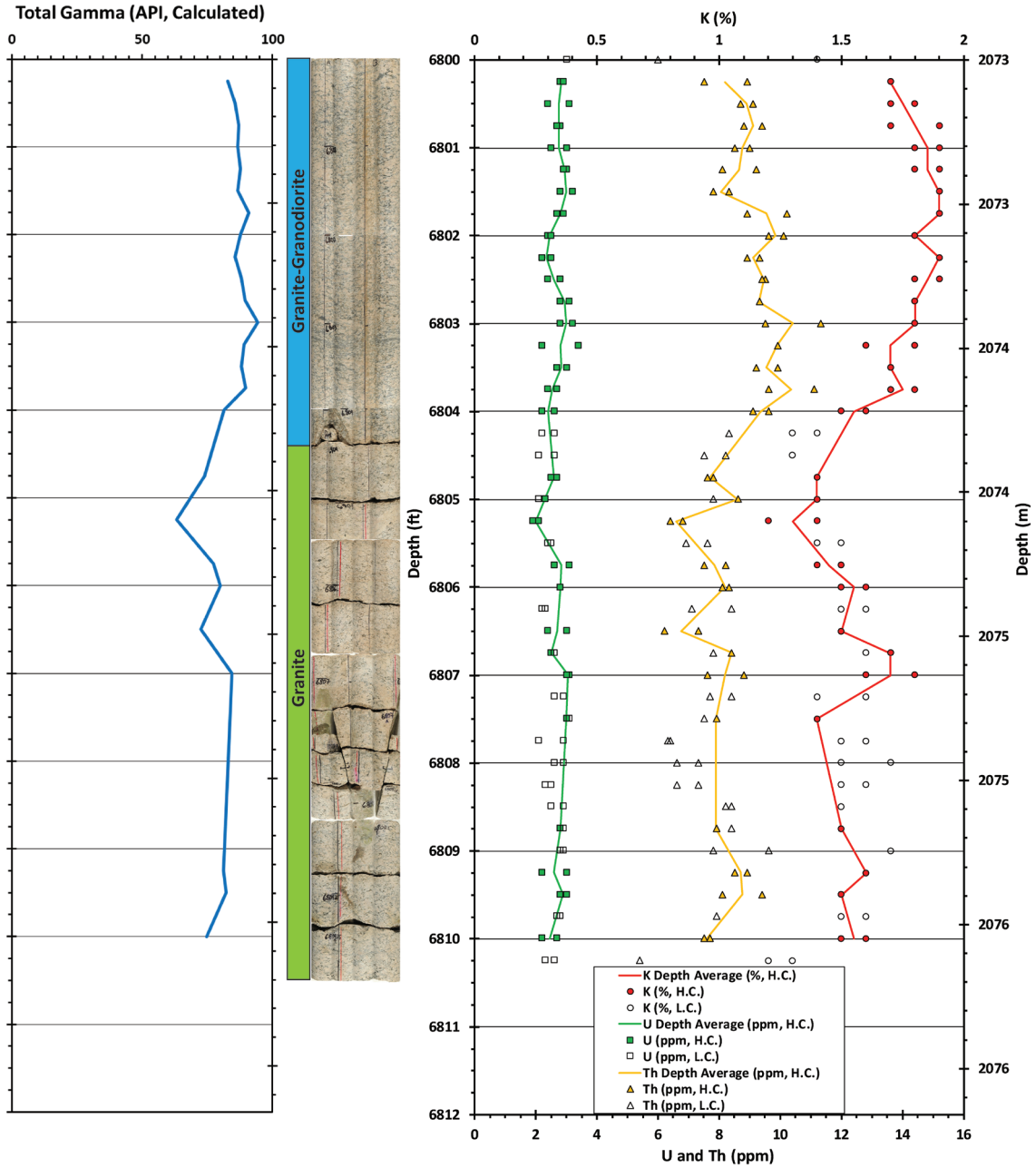

Figure 28. *Spectral gamma-ray measurements in the first cored section of well 58-32 (top at 6800 feet). Two measurements were taken at 3-inch intervals along the reconstructed core, with the measurements taken on opposite sides of the core. Measurements near, or on, fractures were lower confidence (L.C.) due to missing material. However, agreement with high-confidence (H.C.) data suggests the effects are generally moderate. The measurements at each location are plotted, as is the overall average per depth interval (high-confidence data only; colored trend lines). The core was photographed on four sides, and the photos were joined to create the composite photograph in the center. Colored boxes to the left of the photographs indicate rock type (granite-granodiorite and granite) based on XRD analysis of core plugs. Potassium, and to a lesser extent thorium, vary most with changing mineral composition (graph on right). Total gamma was calculated and is shown in the graph at the left. Lower total gamma (and potassium) indicate increasing concentrations of mafic minerals such as biotite, hornblende, augite, titanite, and apatite, and generally correlate with visible changes in lithology. Some areas show significant variation over small depth intervals.*

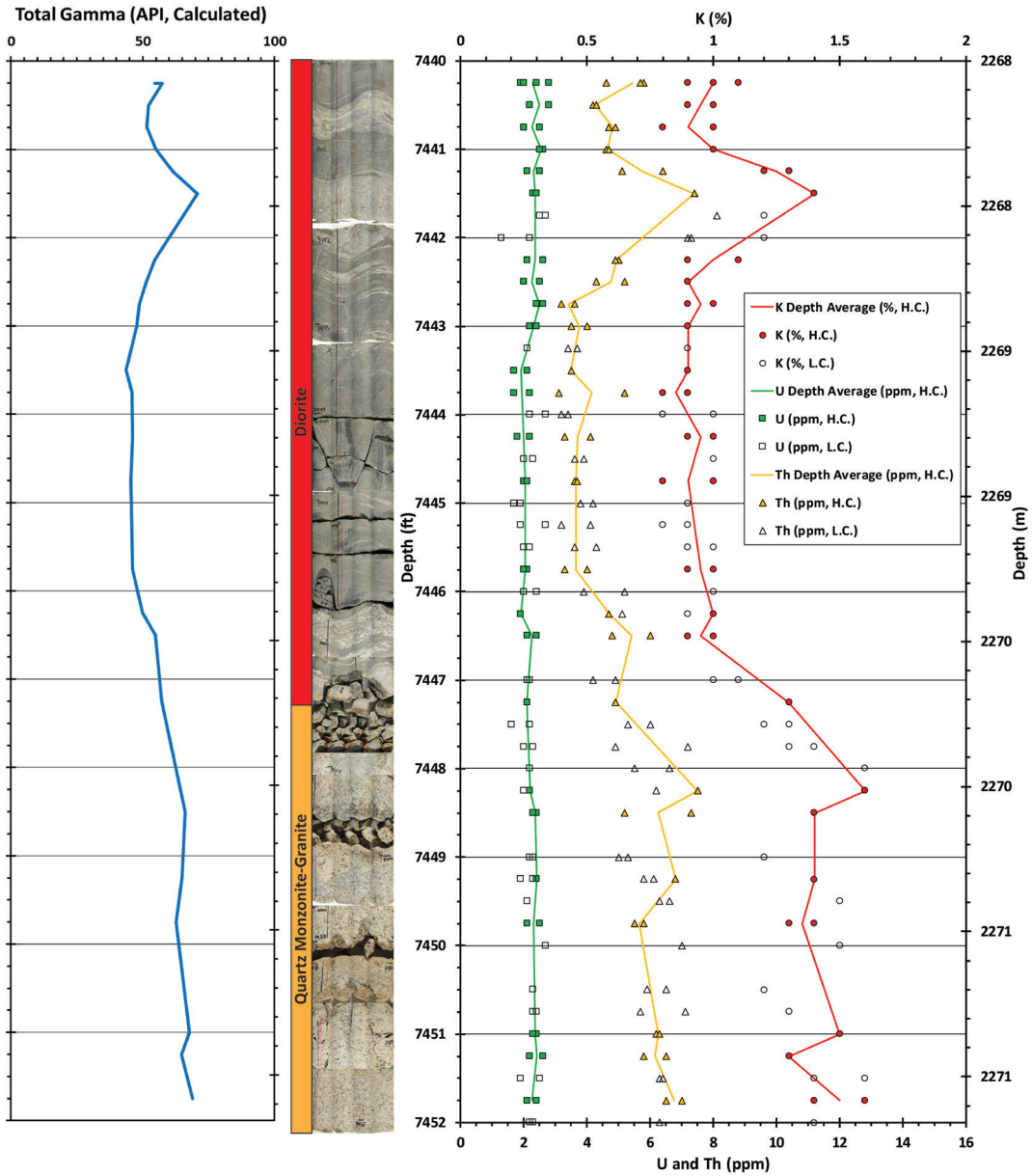

Figure 29. *Spectral gamma-ray measurements in the second cored section of well 58-32 (top at 7440 feet). Two measurements were taken at 3-inch intervals in the reconstructed core, with the measurements taken on opposite sides of the core. Measurements near, or on, fractures were lower confidence (L.C.) due to missing material. However, agreement with high-confidence (H.C.) data suggests the effects are generally moderate. The measurements at each location are plotted, as is the overall average per depth interval (high-confidence data only; colored trend lines). The core was photographed on four sides, and the photos were joined to create the composite photograph in the center. Colored boxes to the left of the photographs indicate rock type (diorite and quartz monzonite-granite) based on XRD analysis of core plugs. Potassium, and to a lesser extent thorium, vary most with changing mineral composition (graph on right). Total gamma was calculated and is shown in the graph at the left. Lower total gamma (and potassium) indicate increasing concentrations of mafic minerals such as biotite, hornblende, augite, titanite, and apatite, and generally correlate with visible changes in lithology (see felsic banding at 7441.6 feet and change from mafic to felsic at about 7446.2 feet). Some areas show significant variation over small depth intervals.*

The MS values in the cores tend to be higher than in the cuttings for a given lithology. Because the instrument is factory-calibrated to measure core of this diameter rather than cuttings, the core values are probably more accurate. The sensitivity of the meter is obvious in the changes from one closely-spaced measurement location to the next in the core. Some of the differences between core and cuttings, therefore, may stem from the cuttings being averaged over 10 feet. An additional factor is likely the decreased density in the cuttings samples, despite the effort to calibrate the instrument for these measurements. While less accurate in an absolute sense, the measurements in the cuttings seem to provide a reasonable representation of relative mineral composition. While there is some overlap, MS values above 30 SI units suggest a dioritic composition and those below that threshold likely have a granitic or intermediate composition.

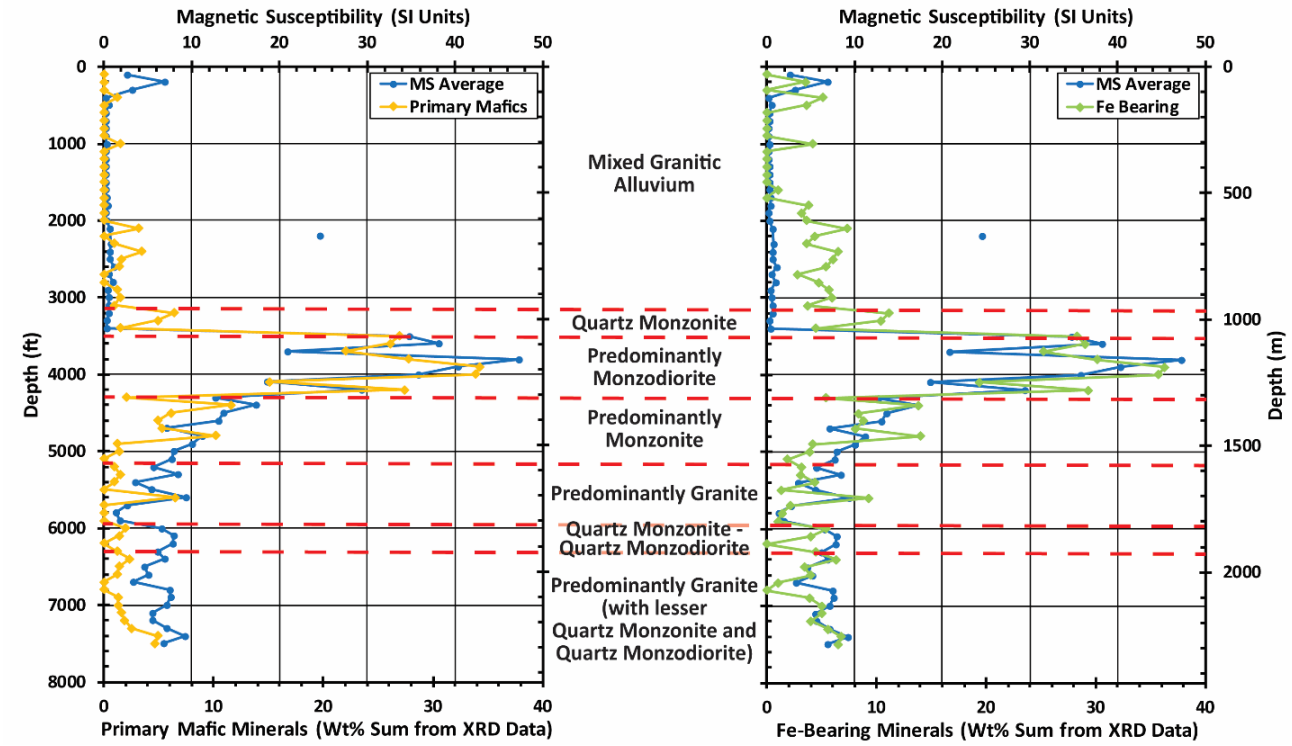

Figure 30. *Magnetic susceptibility (MS) and XRD data (Jones and others, 2018, 2019) for 58-32 well cuttings at 100-foot intervals. The XRD data in the left plot are the sum of the weight percent for primary mafic minerals (biotite, hornblende, augite, titanite, and apatite). The XRD data in the right plot add additional minerals that do, or may, contain iron (smectite, illite, chlorite, and epidote). Both are compared to the XRD-derived predominant rock types. The MS datum at 2200 feet is likely contaminated with steel particles from the drill rig, bit, or casing.*

DETAILED ANALYSIS OF FORGE WELL 58-32 WIRELINE LOGGING DATA

The general calibration of wireline log data (mainly gamma and density) determined by other analyses was used to gain a better understanding of rock characteristics in portions of the 58-32 well bore that were not subject to laboratory analyses. Figures 33 and 34 show the top and bottom halves of the logs shown in Figure 13 so important details can be more easily identified.

Note that the formation density is consistently less than 2.5 g/cm^3 in the alluvial section and that the neutron porosity log shows high (relative to the deeper parts of the well), but decreasing porosity in Figure 33. This is consistent with density measurements on the cuttings. Washouts, identified by spikes in the caliper trace, can significantly affect density calculations, resulting in abnormally low formation density responses (and a deflection of the DRHO trace, which is a measure of density measurement quality). The worst washout zones are highlighted in yellow in Figures 33 and 34. High density/low gamma are indicators of dioritic rock (mainly monzodiorite in Figure 33), which is more common in the upper half of the well.

However, many low density/high gamma peaks that suggest granite, or at least more granitic zones, are present (brown circles in Figure 33). These zones are typically less than 50 feet thick, and many are much thinner. These distinct changes could be the result of magmatic differentiation in the cooling magmas or the result of small intrusions of compositionally different magmas into fractures in existing rock.

The “more granitic” zone near the bottom (about 4200–4300 feet) of the “predominantly monzodiorite” zone, roughly correlates with the quartz monzonite cuttings sampled at 4100–4110 feet. However, most of the other “more granitic spikes” in Figure 33 tend to fall between the XRD-sampled intervals.

The bottom half of the well tends to be more granitic (Figure 34), but small-scale dioritic zones are present. The scale of these zones is generally like the granitic spikes in the upper half of the well. While the only XRD-derived diorite measurement occurred in the lower core (all other dioritic results were monzodiorite), several of the spikes probably reflect “pure” diorite rather than monzodiorite.

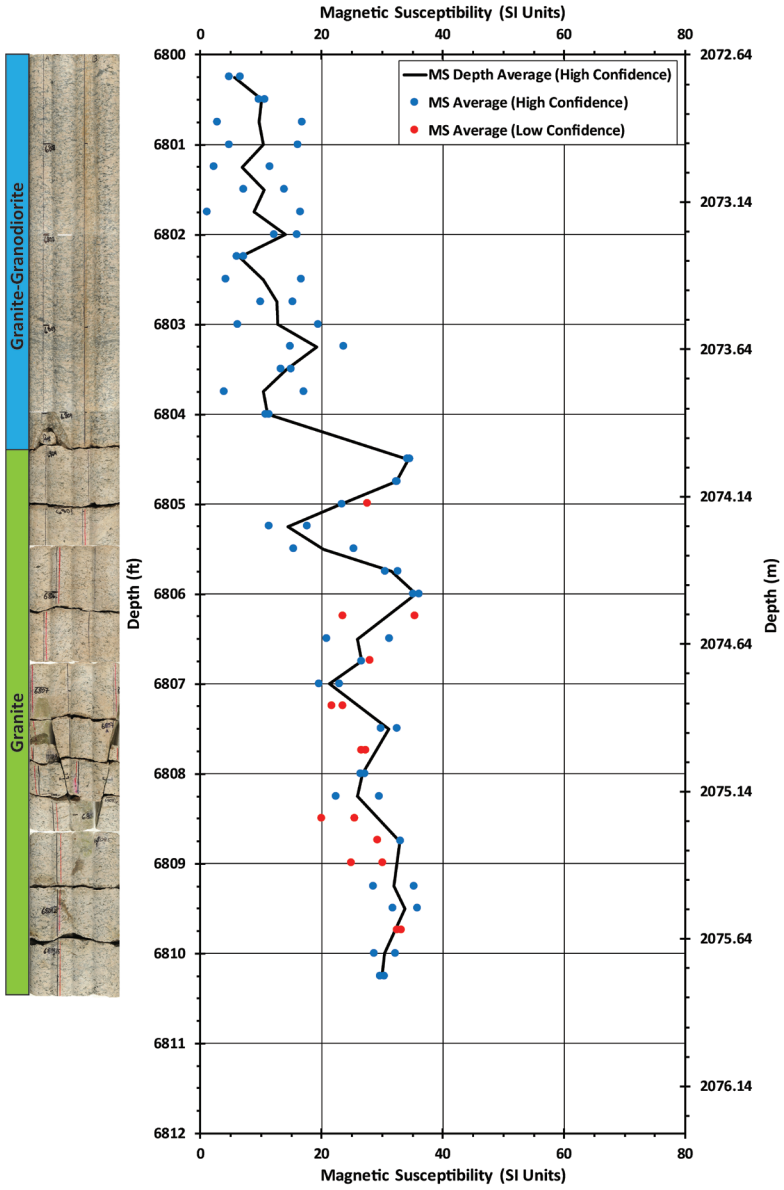

Figure 31. *Magnetic susceptibility (MS) measurements in the first cored section of well 58-32 (top at 6800 feet). Two measurements were taken at 3-inch intervals in the reconstructed core, with each measurement taken on opposite sides of the core. Five measurements were made at each location. Measurements near, or on, fractures were lower confidence due to missing material. However, agreement with high-confidence data suggests the effects are minimal. The average of the five measurements at each location is plotted, as is the overall average per depth interval (high-confidence data only; black trend line). The core was photographed on four sides, and these were joined to create the composite photograph on the left, showing the entire circumference of the core. Colored boxes to the left of the photographs indicate rock type (granite-granodiorite and granite) based on XRD and petrographic studies (Jones and others, 2018, 2019). Higher MS values indicate increasing concentrations of mafic minerals such as biotite, hornblende, augite, titanite, and apatite, and generally correlate with visible changes in lithology. Some areas show significant variation over small depth intervals.*

CONCLUSIONS

The diverse dataset discussed here, along with other data (FMI interpretations, XRD, petrographic studies, etc.) show that the basement rock within the FORGE area consists of a suite of intrusive rock types that are primarily granitic. However, significant quantities of rock with somewhat intermediate compositions (quartz monzonite, monzonite, quartz monzodiorite), and lesser quantities of monzodiorite and diorite are present. The XRD and petrographic data from Jones and others (2018, 2019) show considerable compositional variation with depth through the 58-32 well and reasonably characterize the well in terms of rock type over 100-foot intervals. Log interpretations (primarily based on rock density and the natural gamma signal),

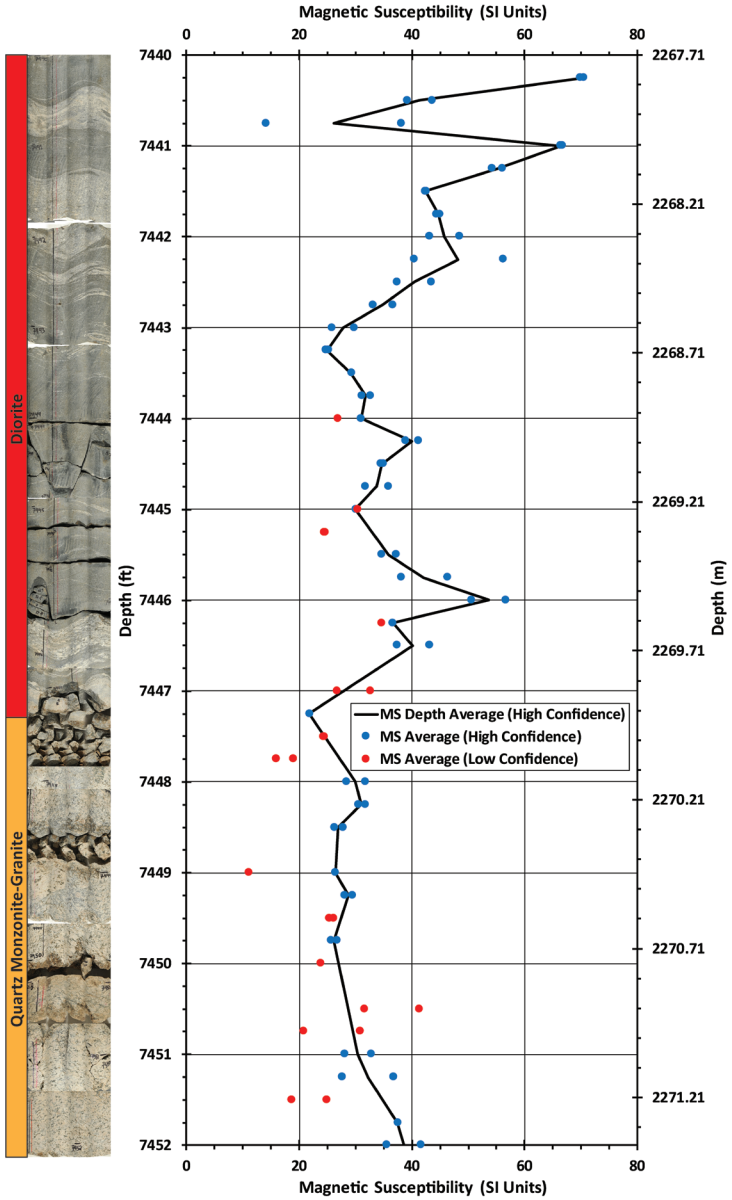

Figure 32. *Magnetic susceptibility (MS) measurements in the second cored section of well 58-32 (top at 7440 feet). Two measurements were taken at 3-inch intervals in the reconstructed core, with each measurement taken on opposite sides of the core. Five measurements were made at each location. Measurements near, or on, fractures were lower confidence due to missing material. However, agreement with high-confidence data suggests the effects are minimal. The average of the five measurements at each location is plotted, as is the overall average per depth interval (high-confidence data only; black trend line). The core was photographed on four sides, and these were joined to create the composite photograph on the left, showing the entire circumference of the core. Colored boxes to the left of the photographs indicate rock type (diorite and quartz monzonite-granite) based on XRD and petrographic studies (Jones and others, 2018, 2019). Higher MS values indicate increasing concentrations of mafic minerals such as biotite, hornblende, augite, titanite, and apatite, and generally correlate with visible changes in lithology. Some areas show significant variation over small depth intervals.*

spectral gamma measurements, thermal conductivity and density measurements, field investigations, and magnetic susceptibility measurements are all in general agreement with the XRD data. The XRD data were used to calibrate many of these other analyses to characterize their results with respect to the specifically identified rock types.

Distinct small-scale changes in rock composition do occur and many of these are missed when looking only at samples from 100-foot intervals. Similar small-scale variations are present in other nearby wells such as 9-1 and 82-33, confirming that such variations are characteristic of the intrusive complex in the FORGE area. These small-scale changes are primarily seen in the log interpretations and in the core analyses, since many of the other types of measurements were made at the same 100-foot intervals as the XRD analyses.

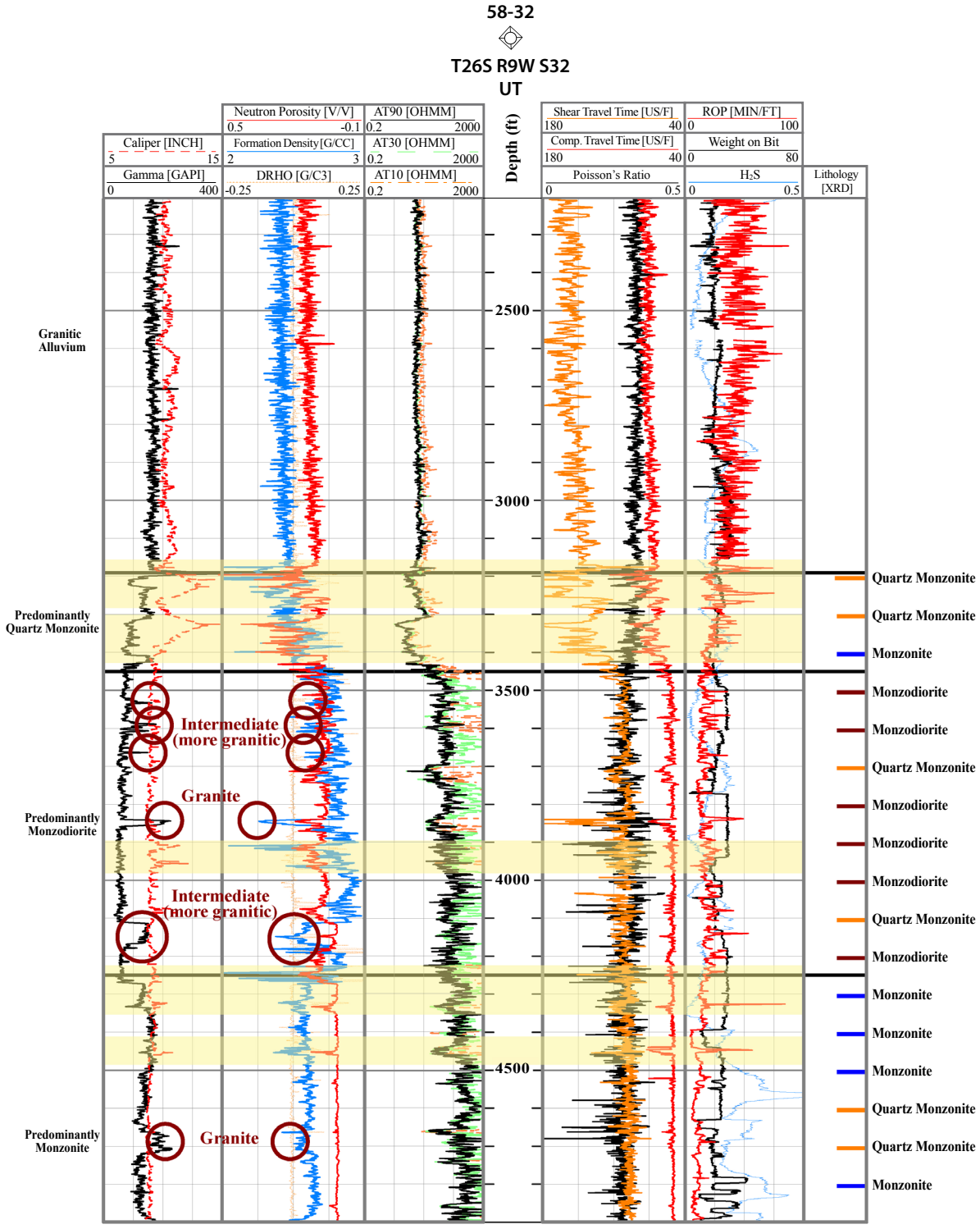

Figure 33. *Selection of wireline log responses for well 58-32 from the bottom of the surface casing at 2173 feet to 4900 feet. "Caliper" indicates hole diameter, "gamma" indicates natural gamma radiation, "neutron porosity" indicates rock porosity, "formation density" indicates rock density, "DRHO" indicates the quality of the density data, "AT__" indicates rock resistivity, "Shear/Comp travel time" and "Poisson's ratio" indicate sonic properties of the formation, "ROP" and "Weight on Bit" indicate drilling parameters, and "H2S" is a measurement of hydrogen sulfide gas released from the formation while drilling. Zones based on gross lithology on the left of the figure are defined by XRD data shown on the right (Jones and others, 2018, 2019). The gamma and formation density curves are the most useful for identifying rock types in the well. High gamma/low density responses are characteristic of granitic rocks while low gamma/high density responses are characteristic of dioritic rocks. Circled "spikes" indicate significant changes in rock composition over a short interval of depth. Most of these "spikes" occur between depths where cuttings were studied and were therefore missed by other analyses. Yellow highlighted zones show where washouts make formation density measurements unreliable (note that much of the "predominantly quartz monzonite" zone was badly affected by washouts). Increasing resistivity from 3300 to 4300 feet suggests weathering.*

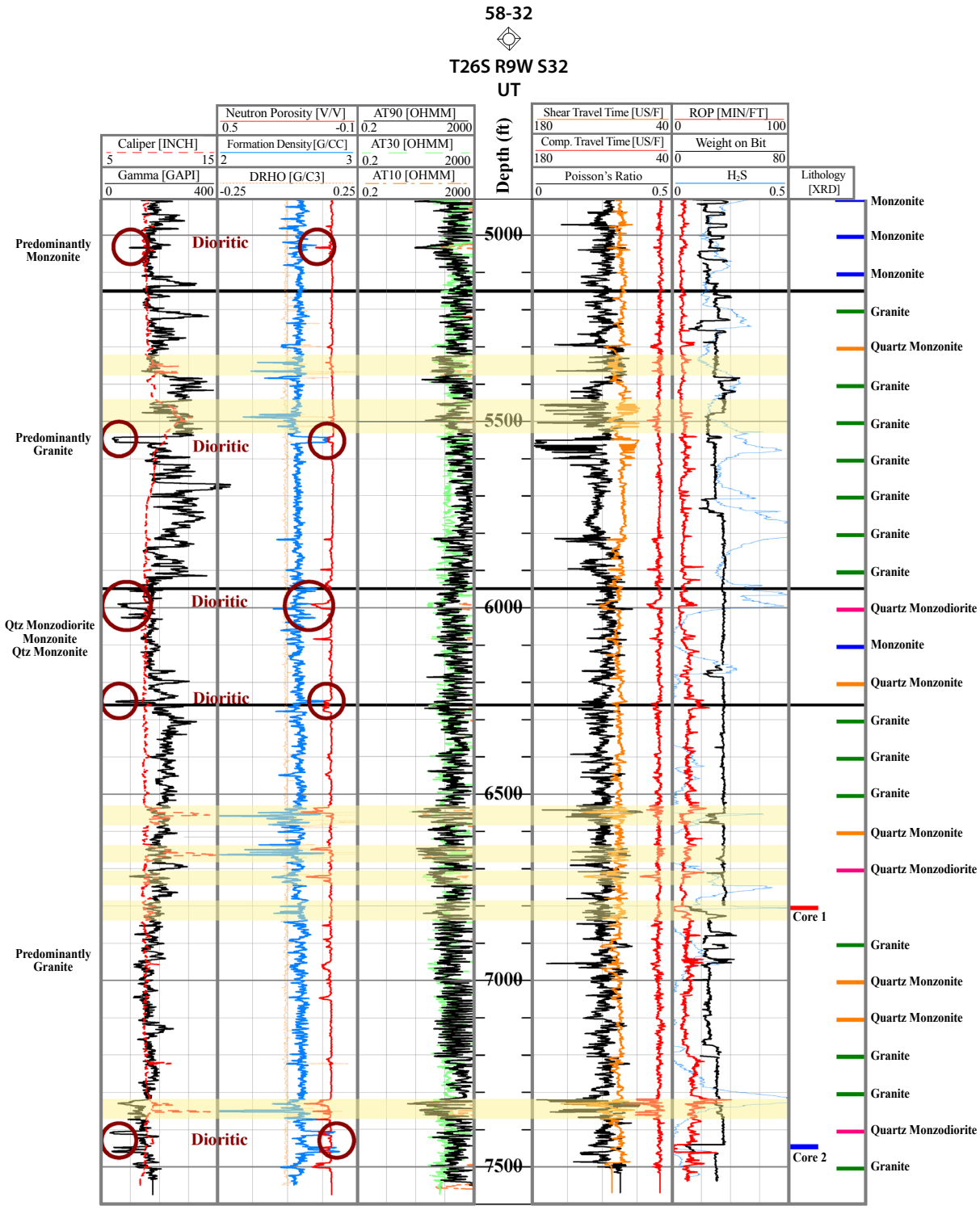

Figure 34. *Selection of wireline log responses for well 58-32 from 4900 feet to 7536 feet (TD). "Caliper" indicates hole diameter, "gamma" indicates natural gamma radiation, "neutron porosity" indicates rock porosity, "formation density" indicates rock density, "DRHO" indicates the quality of the density data, "AT__" indicates rock resistivity, "Shear/Comp travel time" and "Poisson's ratio" indicate sonic properties of the formation, "ROP" and "Weight on Bit" indicate drilling parameters, and "H2S" is a measurement of hydrogen sulfide gas released from the formation while drilling. Zones based on gross lithology on the left of the figure are defined by XRD data shown on the right (Jones and others, 2018, 2019). The gamma and formation density curves are the most useful for identifying rock types in the well. High gamma/low density responses are characteristic of granitic rocks while low gamma/high density responses are characteristic of dioritic rocks. Circled "spikes" indicate significant changes in rock composition over a short interval of depth. Most of these "spikes" occur between depths where cuttings were studied and were therefore missed by other analyses. Yellow highlighted zones show where washouts make formation density measurements unreliable.*

Thermal conductivity measurements provide data that is critical to understanding the thermal regime. These measurements can also help differentiate quartz-rich intrusive rock from other compositions due to the relatively high thermal conductivity of quartz. In 58-32, the matrix thermal conductivity of granite was generally greater than 3.1 W/m°C, while quartz-poor (plagioclase-rich) monzodiorite values were typically around 2.1 to 2.6 W/m°C. Matrix density values are also calculated when performing thermal conductivity measurements, and when adjusted for in situ porosity, may provide better estimates of rock density than density logs because the logs are sensitive to borehole conditions. Density is a major discriminator between dioritic rock (usually about 2.8–3.0 g/cm^3 due to increasing quantities of high-density mafic minerals) and more granitic rock types that are commonly about 2.65–2.75 g/cm^3. Density is not as useful for discerning individual rock types of intermediate composition because variations tend to be small and overlapping.

Spectral gamma measurements should be obtained from the bore hole with a wireline tool to eliminate the uncertainty shown using hand-held instruments at the surface. Wireline surveys with spectral gamma tools are more expensive than those measuring total gamma, but in an intrusive environment where potassium is a major indicator of changing rock type, the results may be worth the added cost. If spectral gamma is not measured as part of a logging package in future wells, the laboratory results could likely be significantly improved with larger cuttings samples, although it may still not be possible to obtain the optimum mass of around 5–6 kilograms. The mass of cuttings samples from the 58-32 well were typically between 300 grams and 700 grams. Because the samples were duplicated for EGI and the UGS, it follows that in wells of similar diameter, samples of around 1.4 kilograms, and possibly much greater, could frequently be collected over a 10-foot drilling interval. If the recovered samples were still below the optimum mass of 5 to 6 kilograms, at least the range of depths required to achieve the optimum mass could be tightened (i.e., maybe 30-foot intervals could be combined rather than the 80-foot intervals as described in this report). Despite the uncertainty of the gamma ray spectrometry measurements in 58-32 (especially in cuttings), Allis and others (2018b) found the relative ratios of potassium, uranium, and thorium to be useful for estimating heat production and differentiating between granitic and dioritic rock types. However, the greatest value of the spectral gamma study in 58-32 could be for the interpretation of down-hole spectral gamma logs if they are obtained in future wells.

Magnetic susceptibility measurements on core samples indicate that small (inch) depth-scale variations in mineral composition do occur. Increasing MS correlates well with increasing quantities of mafic minerals. Cuttings from granite and intermediate rock types that are more quartz-rich in the 58-32 well typically have MS values under 10 SI units, whereas more mafic rocks, particularly monzodiorite and diorite, show values that are typically between 20 and 50 SI units. Because sample measurements can be obtained quickly and inexpensively (now that a calibration has been established for granular materials), they could provide initial insight into rock compositions before more diagnostic analyses such as XRD are performed.

Wireline logs, particularly gamma and density, are key to characterizing the rock penetrated in an intrusive environment such as the FORGE area. They provide data well before laboratory analyses are completed and can highlight important compositional variations that may otherwise be missed by analyses at a coarser range of depths. Like density, total gamma values are less diagnostic of individual intermediate rock types due to overlap. These rock types have a "group" mean of about 150 gAPI, whereas granite has a mean of about 200 gAPI and diorite/monzodiorite has a mean of about 60 gAPI. Wireline spectral gamma logs may help to better differentiate the intermediate rock types in future wells. The log responses that are generally diagnostic of granitic, intermediate, and dioritic rock types are:

- Granitic: Gamma 140–290 gAPI; density about 2.54–2.62 g/cm^3
- Intermediate: Gamma 70–210 gAPI; density about 2.55–2.65 g/cm^3
- Dioritic: Gamma 50–80 gAPI; density 2.65–2.90 g/cm^3

The various analyses of the 58-32 well prove it was drilled into low porosity/low permeability rock that is generally granitic in composition with temperatures well within the DOE-specified window of 175°–225°C. Additionally, despite small-scale compositional changes in the rock, geomechanical characteristics throughout the reservoir zone are reasonably consistent and suitable for testing the techniques and technologies required to develop enhanced geothermal reservoirs.

ACKNOWLEDGMENTS

This work was sponsored by the DOE EERE Geothermal Technologies Office project DE- EE0007080 Enhanced Geothermal System Concept Testing and Development at the Milford City, Utah FORGE Site (Joe Moore, Managing PI). We thank Craig Morgan, David Tabet, Michael Vanden Berg, Kimm Harty, and Mike Hylland for their extensive reviews of this work.

REFERENCES

Ascencio, F., Samaniego, F., and Rivera, J., 2006, Application of a spherical-radial heat transfer model to calculate geothermal gradients from measurements in deep boreholes: Geothermics, v. 35, p. 70–78.

Allis, R., Gwynn, M., Hardwick, C., Hurlbut, W., and Moore, J., 2018a, Thermal characteristics of the FORGE site, Milford, Utah: Transactions, Geothermal Resources Council, v. 42, p. 1011–1025.

Allis, R., Gwynn, M., Hardwick, C., and Moore, J., 2018b, The challenge of correcting bottom-hole temperatures—an example from FORGE 58-32, near Milford, Utah: Proceedings, 43rd Workshop on Geothermal Reservoir Engineering, Stanford University, Stanford, California, SGP-TR-213, 8 p.

Balamir, O., Rivas, E., Rickard, W.M., McLennan, J., Mann, M., and Moore, J., 2018, Utah FORGE reservoir—drilling results of deep characterization and monitoring well 58-32: Proceedings, 43rd Workshop on Geothermal Reservoir Engineering, Stanford University, Stanford, California, SGP-TR-213, 7 p.

Birch, F., and Clark, H., 1940, The thermal conductivity of rocks and its dependence upon temperature and composition: American Journal of Science, v. 238, nos. 8 and 9, p. 529–558 and 613–635.

Blum, P., 1997, Physical properties handbook—a guide to the shipboard measurement of physical properties of deep-sea cores: Ocean Drilling Program Technical Note 26, http://www-odp.tamu.edu/publications/tnotes/tn26/TOC.HTM.

Cenovus Energy, 2014, Hydrogen sulfide (H_2S) Code of Practice, Version 2.0: Cenovus Energy Health and Safety Manual CEN-EHS143, 15 p., https://www.cenovus.com/contractor/health-and-safety-practices.html.

Edwards, M.C., and Chapman, D.S., 2013, Geothermal resource assessment of the Basin and Range province in western Utah—report and heatflow map: Utah Geological Survey unpublished report provided to Arizona Geological Survey under Contract DE-EE0002850, 121 p.

Goutorbe, B., Lucazeau, F., Bonneville, A., 2007, Comparison of several BHT correction methods—a case study on an Australian data set: Geophysical Journal International, v. 170, no. 2, p. 913–922, https://doi.org/10.1111/j.1365-246X.2007.03403.x.

Gwynn, M., Allis, R., Sprinkel, D., Blackett, R., and Hardwick, C., 2014, Geothermal potential in the basins of Northeastern Nevada: Transactions, Geothermal Resources Council, v. 38, p. 1029–1039.

Gwynn, M., Allis, R., Hardwick, C., Jones, C., Nielsen, P., and Hurlbut, W., 2018, Rock properties of FORGE well 58-32, Milford, Utah: Transactions, Geothermal Resources Council, v. 42, p. 1047–1070.

Hardwick, C., Hurlbut, W., Gwynn, M., Allis, R., Wannamaker, P., and Moore, J., 2018, Geophysical surveys of the Milford, Utah, FORGE site—gravity and TEM: Transactions, Geothermal Resources Council, v. 42, p. 1071–1083.

Henrikson, A., and Chapman, D.S., 2002, Terrestrial heat flow in Utah: Unpublished report, University of Utah, http://geology.utah.gov/emp/geothermal/pdf/terrestrialhf.pdf.

Horai, K., and Simmons G., 1969, Thermal conductivity of rock-forming minerals: Earth and Planetary Science Letters, v. 6, p. 359–368.

Jones, C. and Moore, J., 2016, Petrographic and x-ray diffraction analyses of 62 drill cutting samples from geothermal well Accord 1-26, Beaver County, Utah: Unpublished report, Energy & Geosciences Institute at the University of Utah, 23 p.

Jones, C.G., Moore, J.N., and Simmons, S.F., 2018, Lithology and mineralogy of the Utah FORGE EGS reservoir—Beaver County, Utah: Transactions, Geothermal Resources Council, v. 42, p. 1084–1096.

Jones, C.G., Moore, J.N., and Simmons, S., 2019, Petrography of the Utah FORGE site and environs, Beaver County, Utah, *in* Allis, R., and Moore, J.N., editors, Geothermal characteristics of the Roosevelt Hot Springs system and adjacent FORGE EGS site, Milford, Utah: Utah Geological Survey Miscellaneous Publication 169-K, 23 p., 2 appendices, https://doi.org/10.34191/MP-169-K.

Kirby, S.M., Knudsen, T., Kleber, E., and Hiscock, A., 2018, Geologic setting of the Utah FORGE site based on new and revised geologic mapping: Transactions, Geothermal Resources Council, v. 42, p. 1097–1114.

Nadimi, S., Forbes, B., Finnila, A., Podgorney, R., Moore, J., and McLennan, J., 2018, DFIT and fracture modeling of the Utah FORGE site: Transactions, Geothermal Resources Council, v. 42, p. 1144–1154.

OSHA, 2018, Occupational safety and health standards Table Z-2: Occupational Safety and Health Administration, U.S. Department of Labor, https://www.osha.gov/SLTC/hydrogensulfide/standards.html.

Radiation Solutions, 2015, RS-125/230 user manual: Radiation Solutions, Inc., 61 p.

Robertson, E.C., 1988, Thermal properties of rocks: U.S. Geological Survey Open-File Report 88-441, 106 p.

Saint-Gobain, 2016, BGO Bismuth Germanate Scintillation Material: Crystal specifications sheet, Saint-Gobain Ceramics and Plastics, Inc., 2 p., https://www.crystals.saint-gobain.com/products/bgo.

Sibbett, B.S., and Nielsen, D.L., 2017, Geologic map of the central Mineral Mountains, Beaver County, Utah (GIS reproduction of 1980 map): Utah Geological Survey Map MP-17-2dm, 1:24,000.

Whittington, A., Hofmeister, A., and Nabelek, P., 2009, Temperature-dependent thermal diffusivity of the Earth's crust and implications for magmatism: Nature, v. 458, p. 319–321.